

Investigation of microbicidal activity of surface-immobilized hydrophobic polycations

by

Bryan Boen Hsu

B.S., Chemical Engineering (2007)
B.S., Materials Science and Engineering (2007)

University of California, Berkeley

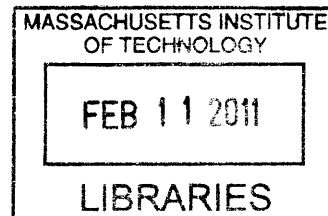
Submitted to the Department of Chemistry
in Partial Fulfillment of the Requirements for the Degree of
Master of Science in Chemistry

at the

Massachusetts Institute of Technology

February 2011

© 2011 Massachusetts Institute of Technology
All rights reserved



ARCHIVES

Signature of Author _____

Department of Chemistry
January 11, 2011

Certified by _____

Alexander M. Klibanov
Novartis Professor of Chemistry and Bioengineering
Thesis Advisor

Accepted by _____

Robert W. Field
Chairman, Department Committee on Graduate Students

Investigation of microbicidal activity of surface-immobilized hydrophobic polycations

by

Bryan Boen Hsu

Submitted to the Department of Chemistry
on January 11, 2011 in Partial Fulfillment of the
Requirements for the Degree of Master of Science in
Chemistry

ABSTRACT

Hydrophobic polycations have been shown to completely kill bacterial, fungal, and viral pathogens, on-contact. Herein we describe advances with this technology on two fronts: (1) innovation of a polycationic-derivative that simplifies the labor-intensive covalent-immobilization procedure, and (2) elucidation of the current mechanistic understanding of this phenomenon.

First, we developed and characterized a novel polycationic polymer capable of cross-linking to cotton *via* activation with ultraviolet light. The resultant, covalently-immobilized, *N*-alkyl polyethylenimine (PEI) demonstrates complete bactericidal activity against *S. aureus* and *E. coli* (i.e., representative Gram-positive and Gram-negative bacteria, respectively). In addition, by utilizing light to activate the covalent cross-linking, this immobilization procedure is simpler and more versatile than similar chemically-attached bactericidal polycations.

Second, we shed light onto how the coating inactivates microbial pathogens. Gram-negative and Gram-positive bacteria exposed to the polycationic coating revealed substantial structural deformation, which allowed for the leakage of their intracellular contents. Characterization of the enzymes leaked into solution from Gram-negative bacteria indicated a disproportionately greater damage done to the outer-membrane than the inner-membrane. In addition, the quantity of proteins leaked into solution showed striking similarity to results obtained from bacteria subjected to lysozyme/EDTA treatment (i.e., a traditional cell lysis technique that degrades the cellular wall). In total, these results suggest that it is this interaction between the polycation and cellular structure (i.e., outer membrane and cell wall) that ultimately compromises bacterial integrity. Expanding our investigation, we studied the effect of the polycationic coating on another membrane-enclosed microbe: the influenza virus. We found that the viral particles adhere to the polycationic coating, which results in a structural deformation, similar to that borne-out by bacteria. As a consequence, viral genomic material is leaked into solution, revealing the viruses' state of inactivation upon adherence to the coating.

Thesis Supervisor: Alexander M. Klibanov

Title: Novartis Professor of Chemistry and Bioengineering

TABLE OF CONTENTS

<u>Section</u>	<u>Page</u>
Chapter 1. Brief review of antimicrobial surfaces	
1.1 Introduction.....	4
1.2 References.....	7
Chapter 2. Light-activated covalent coating of cotton with bactericidal hydrophobic polycations	
2.1 Introduction.....	9
2.2 Results and Discussion.....	10
2.3 Conclusions.....	20
2.4 Materials and Methods.....	21
2.5 References.....	25
Chapter 3. On structural damage incurred by bacteria upon exposure to hydrophobic polycationic coatings	
3.1 Introduction.....	26
3.2 Results and Discussion.....	27
3.3 Conclusions.....	35
3.4 Materials and Methods.....	36
3.5 References.....	40
Chapter 4. On the mechanism of inactivation of influenza viruses by immobilized hydrophobic polycations	
4.1 Introduction.....	41
4.2 Results and Discussion.....	43
4.3 Conclusions.....	57
4.3 Materials and Methods.....	58
4.4 References.....	65
Appendix I. Efficacy of ribonuclease and its subsequent inhibition.....	67
Acknowledgements	69

Chapter 1: Brief review of antimicrobial surfaces

1.1 Introduction

Communicable diseases are a major public health threat and the leading cause of death in children worldwide (1). They contribute significantly to nosocomial infections in hospitals through contaminated staff, surfaces, and medical devices (2, 3). Populations of developing nations are particularly vulnerable to pathogenic microbes because of inferior municipal infrastructures and standards of living (4); their implementation of existing technologies to combat transmission of these diseases often fails due to limited resources (5).

Compounding this issue is the increasing frequency with which human-pathogenic microbes develop resistances to commonly used disinfectants and antimicrobials. A combination of factors, including genetic mutations and improper/over-usage of chemicals, have been suspected as the cause of developed resistances (6). Unfortunately, scientific response has been slow because the main avenue to overcoming drug-resistance, namely development of new drugs, is often slow to bear fruit (7).

One complementary approach to combating microbial infections is to kill the pathogens before their contact with the human body. Transmission of communicable diseases commonly occurs by touching contaminated surfaces in high-traffic areas such as doorknobs, keyboards and elevator buttons. Even in the health-care setting, where sanitation is of paramount importance, microbes can be easily transmitted between patients by hospital staff (8). Tackling this issue is even more critical with regard to implant-related infections, where the material's surface can provide a suitable environment for microbial cultivation (9). Traditionally, surfaces are disinfected by wipe-downs with a microbicidal solution (e.g. ethanol, bleach, or benzalkonium

chloride), which can briefly decontaminates the surface. Unfortunately this is only temporarily effective, as microbes can later recolonize the surface. A number of alternatives including TiO₂ photocatalysts (10), Ag ions (11), antimicrobial peptides (12), and time-release antibiotics (13)—among others (9)—have been explored but each retains some significant drawback ranging from requiring activation for microbicidal effect, to leaching, and to potency towards only a narrow-spectrum of microbes.

Polymerized quaternary ammonium compounds have shown a unique blending of desirable characteristics. Both polyethylenimine (PEI) and poly(vinylpyridine) (PVP) based hydrophobic polycations have demonstrated microbicidal activity that upon deposition requires no subsequent “activation”, remains permanently microbicidal (i.e., is still microbicidal after repeated challenges), can be “refreshed” with routine washing, and demonstrates a broad-spectrum efficacy against a multitude of microbes (14). In addition, there is preliminary *in vitro* data that suggests this type of coating may be non-toxic to mammalian cells (15, 16).

Understanding how hydrophobic polycations are able to inactivate microbial pathogens is key to its potential incorporation into multifunctional technologies and widespread use. Fortunately there is preliminary mechanistic evidence, specifically regarding the polymer’s properties. For example, the length (i.e., hydrophobicity) of the pendant alkyl chain in *N*-alkyl-PVP and *N,N*-alkyl,methyl-PEI shows a minimum hydrophobicity is necessary for bactericidal activity (17, 18). In addition, the PEI-based polymer reveals that increasing the polycationic charge (18) and the overall polymer molecular weight (19) enhances bactericidal activity as well.

The biological properties affected by hydrophobic polycations are not so well understood. Thus far, a wealth of information has been collected describing the broad spectrum of microbes

susceptible to these coatings, ranging from bacteria to fungi and viruses (14). The microbicidal polymer is proposed to incur damage to the biological membrane, which is a shared feature among the tested microbes. Previous mechanistic studies have shown that their membranes are damaged, such that normally non-permeable small molecule dyes can now pass through (15, 20), but the extent of damage is not completely understood.

In building upon this knowledge, we made advances in this field on two fronts. First we developed a hydrophobic polycation that covalently cross-links to cotton upon activation with light (21). Then we found that upon contact with the hydrophobic polycations, bacteria (*Escherichia coli* and *Staphylococcus aureus*) were significantly damaged, releasing their intracellular contents (22). This was not limited to bacteria, since we have also found that influenza viruses are considerably damaged, releasing their genomic material (23).

1.2 References

1. Bryce J, Boschi-Pinto C, Shibuya K, Black RE (2005) WHO estimates of the causes of death in children. *Lancet* 365:1147-1152.
2. Rosenthal VD, *et al.* (2006) Device-associated nosocomial infections in 55 intensive care units of 8 developing countries. *Ann Intern Med* 145:582-591.
3. Boyce JM, Potter-Bynoe G, Chenevert C, King T (1997) Environmental contamination due to methicillin-resistant *Staphylococcus aureus*: Possible infection control implications. *Infect Cont Hosp Ep* 18:622-627.
4. Harris E (2004) Building scientific capacity in developing countries. *EMBO Rep* 5:7-11.
5. Madu CN (1989) Transferring technology to developing countries - critical factors for success. *Long Range Plann* 22:115-124.
6. Gold HS, Moellering RC (1996) Drug therapy - Antimicrobial-drug resistance. *N Engl J Med* 335:1445-1453.
7. Spellberg B, Powers JH, Brass EP, Miller LG, Edwards JE (2004) Trends in antimicrobial drug development: Implications for the future. *Clin Infect Dis* 38:1279-1286.
8. Pittet D, Allegranzi B, Sax H, Dharan S, Pessoa-Silva CL, Donaldson L, Boyce JM (2006) Evidence-based model for hand transmission during patient care and the role of improved practices. *Lancet Infect Dis* 6:641-652.
9. Hetrick EM, Schoenfisch MH (2006) Reducing implant-related infections: active release strategies. *Chem Soc Rev* 35:780-789.
10. Sunada K, Kikuchi Y, Hashimoto K, Fujishima A (1998) Bactericidal and detoxification effects of TiO₂ thin film photocatalysts. *Environ Sci Technol* 32:726-728.
11. Sondi I, Salopek-Sondi B (2004) Silver nanoparticles as antimicrobial agent: a case study on *E. coli* as a model for Gram-negative bacteria. *J Colloid Interf Sci* 275:177-182.
12. Brogden KA (2005) Antimicrobial peptides: Pore formers or metabolic inhibitors in bacteria? *Nat Rev Microbiol* 3:238-250.
13. Zilberman M, Elsner JJ (2008) Antibiotic-eluting medical devices for various applications. *J Control Release* 130:202-215.
14. Klibanov AM (2007) Permanently microbicidal materials coatings. *J Mater Chem* 17:2479-2482.
15. Milovic NM, Wang J, Lewis K, Klibanov AM (2005) Immobilized *N*-alkylated polyethylenimine avidly kills bacteria by rupturing cell membranes with no resistance developed. *Biotechnol Bioeng* 90:715-722.
16. Mukherjee K, Rivera JJ, Klibanov AM (2008) Practical aspects of hydrophobic polycationic bactericidal "paints". *Appl Biochem Biotechnol* 151:61-70.
17. Tiller JC, Liao CJ, Lewis K, Klibanov AM (2001) Designing surfaces that kill bacteria on contact. *Proc Natl Acad Sci USA* 98:5981-5985.
18. Lin J, Qiu SY, Lewis K, Klibanov AM (2002) Bactericidal properties of flat surfaces and nanoparticles derivatized with alkylated polyethylenimines. *Biotechnol Prog* 18:1082-1086.
19. Lin J, Qiu SY, Lewis K, Klibanov AM (2003) Mechanism of bactericidal and fungicidal activities of textiles covalently modified with alkylated polyethylenimine. *Biotechnol Bioeng* 83:168-172.

20. Park D, Wang J, Klivanov AM (2006) One-step, painting-like coating procedures to make surfaces highly and permanently bactericidal. *Biotechnol Prog* 22:584-589.
21. Hsu BB, Klivanov AM (2010) Light-activated covalent coating of cotton with bactericidal hydrophobic polycations. *Biomacromol* In Press.
22. Hsu BB, Ouyang J, Wong SY, Hammond PT, Klivanov AM (2010) On structural damage incurred by bacteria upon exposure to hydrophobic polycationic coatings. *Biotechnol Lett* In Press.
23. Hsu BB, Wong SY, Hammond PT, Chen J, Klivanov AM (2010) Mechanism of inactivation of influenza viruses by immobilized hydrophobic polycations. *Proc Natl Acad Sci USA* In Press.

Chapter 2. Light-activated covalent coating of cotton with bactericidal hydrophobic polycations

2.1 Introduction

Biocidal materials can be created by impregnating, adsorbing, or covalently attaching to their surfaces of microbicidal agents (1, 2). We have employed the last approach by covalently immobilizing *N*-alkylated poly(vinyl pyridines) and polyethylenimines (PEIs), thus making them permanently microbicidal and non-leaching (3-5). However, this procedure requires a multi-step and surface-specific immobilization and may be problematic for large-scale applications. To address this issue, we also have developed an alternative procedure, whereby surfaces are non-covalently coated by hydrophobic polycations, e.g., *N,N*-dodecyl,methyl-PEI (6). This “painting”, while simple, is potentially liable to environmental deterioration (7).

Herein we describe the next generation microbicidal coating that combines the permanence and resilience of covalent attachment with the ease of painting. The new photosensitive hydrophobic polycationic salt can be synthesized elsewhere and then shipped to a field location for a simple coating procedure requiring no skilled personnel. Ultraviolet (UV) light was selected as the immobilization trigger because of its simplicity and abundance of sunlight in most developing countries. As described below, a cotton fabric is simply soaked in a solution of a designed *N*-alkyl-PEI, followed by a UV irradiation, to result in a permanently bactericidal textile.

2.2 Results and Discussion

We selected branched PEI (**1**) as the starting point of our polycationic coating because of its high amine density and a 1:2:1 ratio of primary, secondary, and tertiary amino groups (**8**). Our previous studies (**1**) have revealed that high microbicidal activity requires not only high positive charge but also substantial hydrophobicity (i.e., alkyl chain length) (**6**, **9**). For photo cross-linking, we chose an aryl azide group with a ~1.8-nm spacer arm because of its extension beyond proximal alkyl groups and preferential reactivity toward nucleophiles (**10**), such as cellulosic –OH groups.

To this end, we derivatized the primary amino groups (**11**) of **1** with a stoichiometrically small fraction of trityl chloride (Scheme 2.1), which yielded **2** with some 2% of the total amines protected. Subsequent alkylation of the free amino groups of **2** with 1-bromododecane yielded **3**. In preparation for the photo cross-linker 6-(4'-azido-2'-nitrophenylamino)hexanoyl (ANPAH), **3** was deprotected under acidic conditions to give **4**, whose primary amines were reacted with the NHS-ester precursor of ANPAH to produce **5**. Positive charges were maximized by methylating the nucleophilic amino groups into quaternary ammonium groups, yielding the final photosensitive polymer **6** (Fig. 2.1A). Plain cotton fabric was then dipped into a 50 mg/mL solution of **6** in CH₂Cl₂ (Fig. 2.1B), dried in the dark, and derivatized by exposure to UV light, followed by thorough washing with fresh CH₂Cl₂. Comparison of plain cotton (Fig. 2.1C) with that **6**-photocoated thrice (Fig. 2.1D) shows the latter's yellow color and thus qualitatively confirms the coating.

Scheme 2.1. The synthetic scheme for making of *N,N,N*-ANPAH,dodecyl,methyl-PEI (**6**). The abbreviated chemical groups are trityl (triphenylmethyl, Tr) and 6-(4'-azido-2'-nitrophenylamino)hexanoyl (ANPAH). See Materials and Methods for details.

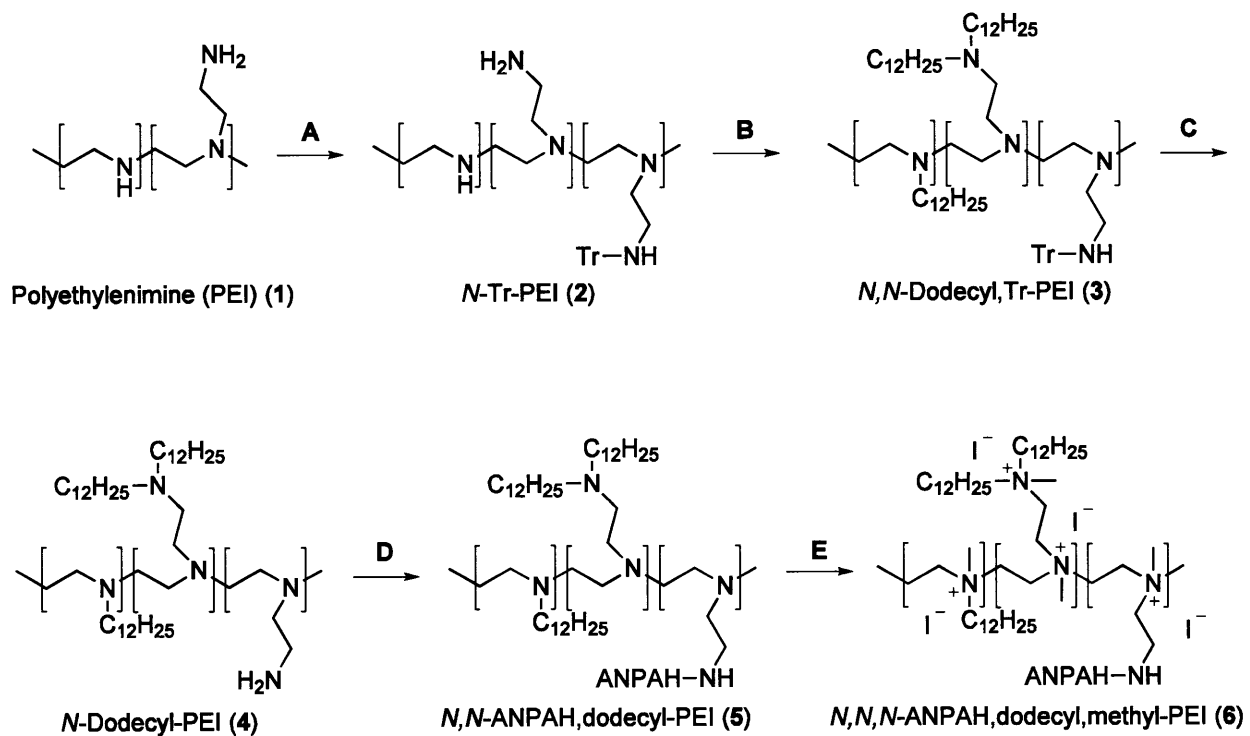
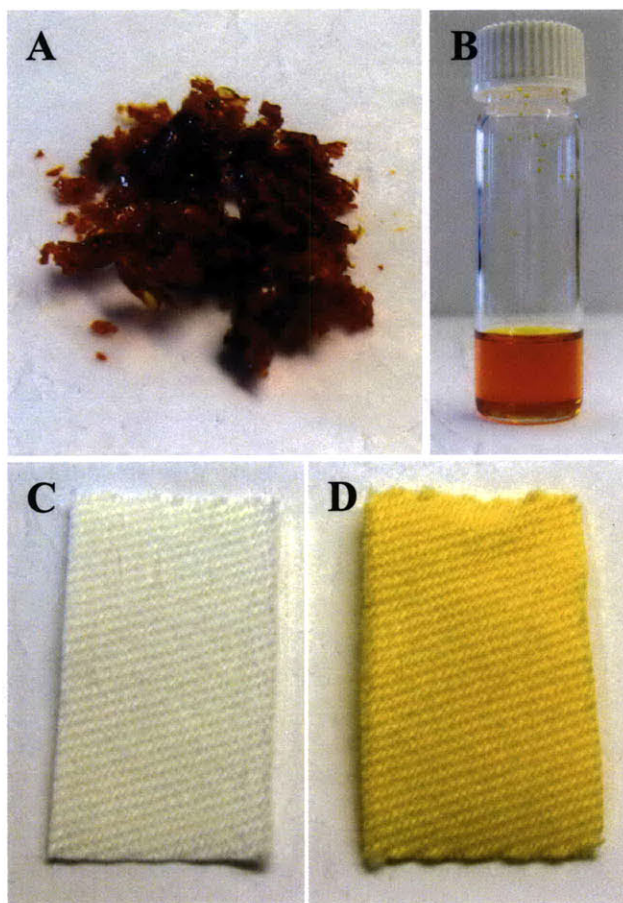


Figure 2.1. The *N,N,N*-ANPAH,dodecyl,methyl-PEI (**6**) prepared by us herein is shown as a solid (A) and as a 50 mg/mL solution in CH₂Cl₂ (B). Plain and **6**-photocoated cotton samples are depicted in (C) and (D), respectively. See Materials and Methods for details.



For characterization of the coated surface, we used X-ray photoelectron spectroscopy (XPS). Elemental analysis of plain cotton (first row of Table 2.1) shows significant quantities of carbon, oxygen, and calcium (the Ca is likely a residual contaminant from the manufacturer's washing procedure (12)). The measured C/O ratio of 1.22 agrees well with the theoretical value of 1.20 for cellulose ($C_6H_{10}O_5$)_n. In comparison, the elemental composition of the **6**-photocoated cotton (second row of Table 2.1) reveals substantial quantities of nitrogen and iodine, as well as over a 2-fold jump in the C/O ratio to 2.72, confirming the presence of covalently immobilized **6**.

To quantify the polymer on the surface, we titrated the quaternary ammonium groups with fluorescein (3). While the plain cotton showed only a low, non-specific fluorescein absorption of 0.14 ± 0.02 nmol/cm², the **6**-photocoated cotton exhibits nearly a 100-fold greater value (first column, second row of Table 2.2). To put this value in perspective, we compared and found it to be similar with that for covalently immobilized *N,N*-hexyl,methyl-PEI (first row of column 1 in Table 2.2). Separately, previous studies (9) with branched *N,N*-alkyl,methyl-PEI (with alkyl being hexyl or dodecyl) covalently immobilized on glass found somewhat lower levels of *N*-quaternization (column 2 of Table 2.2). The overall lesser density of the latter on glass is likely due to cotton's greater surface roughness.

Table 2.1. The elemental surface-compositions of plain cotton and of that 6-photocoated thrice, as determined by means of X-ray photoelectron spectroscopy (XPS).

Sample	Elemental composition (atomic %)				
	C	O	N	Ca	I
Plain cotton	54.4	44.5	<i>N.D.</i>	1.1	<i>N.D.</i>
6-Photocoated cotton	71.0	26.1	1.8	<i>N.D.</i>	1.1

N.D.: Not Detectable (i.e., < 0.5 atomic %) (13)

Table 2.2. The quaternary ammonium group densities of branched *N*-alkyl-PEIs covalently immobilized onto glass slides and cotton fabric.

Alkyl group	Quaternary ammonium group density (nmol/cm ²)	
	Cotton	Glass
Hexyl (C ₆)	17.3 ± 0.4 ^a	6.8 ± 1.9 ^c
Dodecyl (C ₁₂)	11.0 ± 0.9 ^b	4.8 ± 1.5 ^c

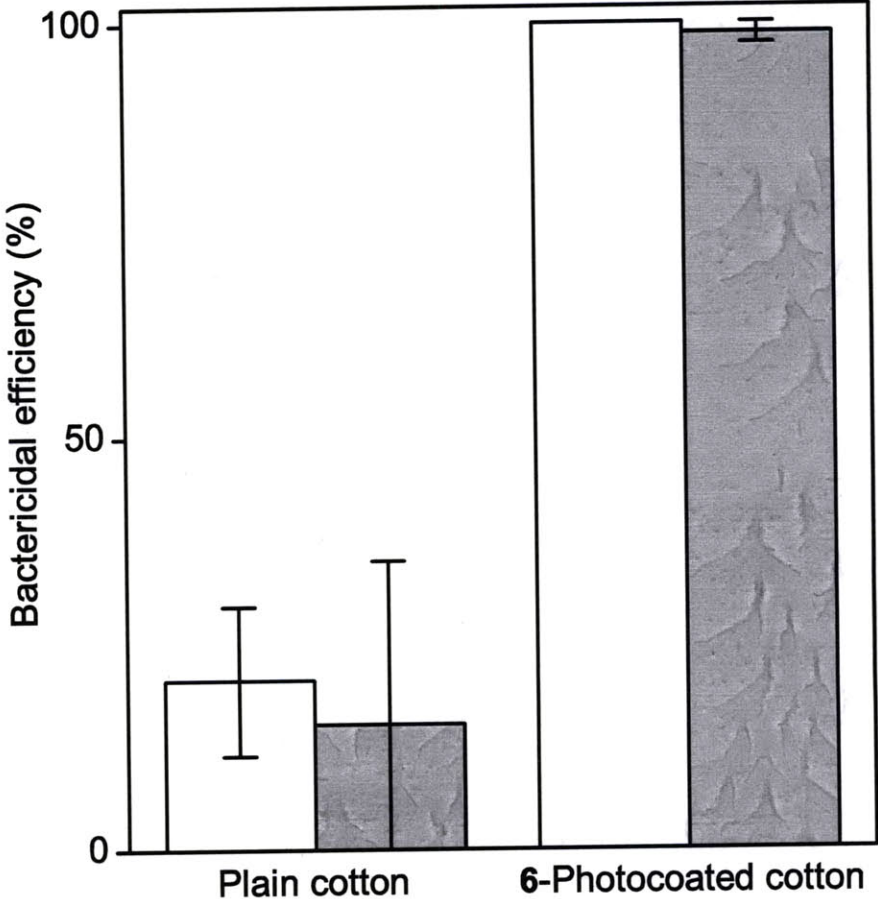
^aCovalently derivatized with *N,N*-hexyl,methyl-PEI; see ref. (3).

^bCovalently photocoated with **6**.

^cCovalently derivatized with *N,N*-alkyl,methyl-PEI; see ref. (9).

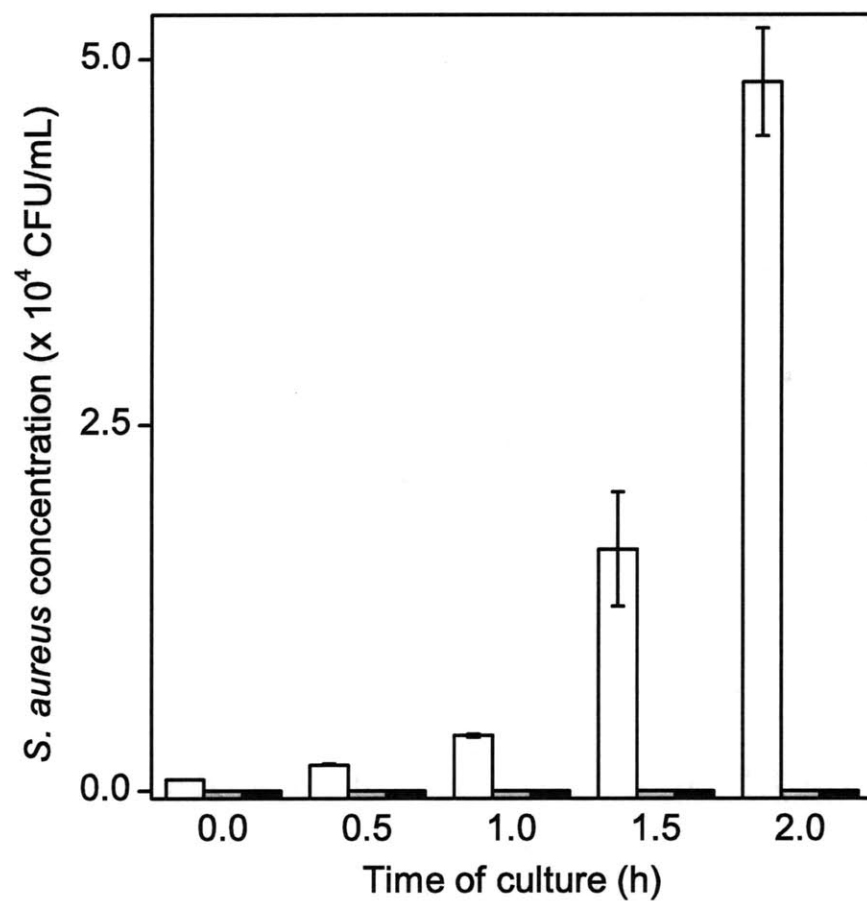
The ultimate merit of the photocoating procedure developed herein rests on how bactericidal the treated cotton fabric becomes. We addressed that issue with representative waterborne human pathogenic bacteria, *E. coli* and *S. aureus* (Gram-negative and Gram-positive, respectively) using two different tests. Under our assay conditions, 195 ± 22 and 92 ± 13 colony-forming units (CFU) were observed in plated 5-fold serial dilutions of *E. coli* and *S. aureus* suspensions, respectively. Upon incubation of the bacteria with plain cotton, their titers were only slightly reduced (Figure 2.2), presumably due to entrapment of some bacteria within the cotton fibers. However, following the same incubation with 6-photocoated cotton, essentially no viable bacteria were detected (Fig. 2.2).

Figure 2.2. Waterborne bactericidal efficiencies of plain cotton (the left pair of bars) and of that photocoated with 6 (the right pair of bars) against *E. coli* (white bars) and *S. aureus* (gray bars).



We elaborated on this finding further in another test by assessing the viability of bacteria adhered to the cotton samples. Immediately after the waterborne bactericidal assay with *S. aureus*, we transferred the tested cotton samples into fresh media and monitored the bacterial concentration under growth conditions. As a positive control, we included cotton derivatized with covalently-immobilized *N,N*-hexyl,methyl-PEI, which had undergone identical bacterial treatment and showed 100% bactericidal activity against waterborne *S. aureus*. As seen in Figure 2.3, there was vigorous bacterial growth on plain cotton, indicating that the bacteria adhered to, or entrapped within, the cotton fibers remain viable. In contrast, both the *N,N*-hexyl,methyl-PEI-derivatized and 6-photocoated cotton samples exhibited no significant concentrations of bacteria over the same 2-h period, indicating that their surfaces inactivated the cells adhered to them. These observations are consistent with our previous studies showing that hydrophobic polycations covalently immobilized (14) or “painted” (6) onto solid surfaces kill bacteria on contact.

Figure 2.3. Replicative ability of *S. aureus* adhered to plain cotton (white bars), *N,N*-hexyl,methyl-PEI-derivatized cotton (gray bars), and 6-photocoated cotton (black bars) after a waterborne bactericidal assay. See Materials and Methods for details.



2.3 Conclusions

Herein we have designed and synthesized a photosensitive *N*-alkyl-PEI that shares the permanence of covalently attached hydrophobic polycations but is applied as easily as painting. The imbedded polymer can be cross-linked to a cotton fabric in a simple procedure triggered by UV light with the resultant quaternization densities and, importantly, bactericidal efficiencies similar to those in the previously described labor-intensive and multi-step covalent attachment procedure.

2.4 Materials and Methods

Synthesis

Unless otherwise noted, all chemicals were from Sigma-Aldrich Chemical Co. and used without further purification. All ^1H NMR spectra were obtained with a Varian Inova-500 spectrometer.

As shown in Scheme 2.1A, following drying under vacuum for 3 days, 1.6 g of branched PEI (**1**) ($M_w = 750$ kDa) was dissolved in 7.7 mL of anhydrous *N,N*-dimethylformamide with ultrasonication. After stirring with an additional 1.8 mL of anhydrous CH_2Cl_2 and 120 μL of *N,N*-diisopropylethylamine for 30 min at room temperature, 1.8 mL of 0.5 M trityl (Tr) chloride in anhydrous CH_2Cl_2 was added dropwise at -10°C in a NaCl/ice bath under argon (11, 15). This mixture was stirred and returned to room temperature over 20 h to yield a white precipitate. The volatiles were removed under vacuum, and the precipitate was dissolved in CH_3OH and dialyzed twice from a regenerated cellulose membrane bag (Spectrum Labs, 3.5-kDa MWCO) against 1 L of CH_3OH at room temperature for 18 h. After solvent removal under vacuum, the yield of *N*-Tr-PEI (**2**) was 1.2 g, with 2.2% of the amino groups tritylated. ^1H NMR (500 MHz, CD_3OD , δ): 2.25-3.00 (br, 4H, $-\text{NCH}_2\text{CH}_2-$), 7.09 (s, 2H, *ortho*-Ar), 7.18 (s, 1H, *para*-Ar), 7.35 (s, 2H, *meta*-Ar).

As shown in Scheme 2.1B, **2** was dissolved in 15 mL of *tert*-amyl alcohol and stirred with 4.6 g of K_2CO_3 and 20 mL of 1-bromododecane at 95°C for 96 h (6, 16). After cooling to room temperature and centrifugation at 6,000 rpm for 30 min, the supernatant was dialyzed twice against 2 L of hexane for 18 h. The solvent was removed under vacuum, and the yield of *N,N*-dodecyl,Tr-PEI (**3**) was 6.0 g. ^1H NMR (500 MHz, CD_2Cl_2 , δ): 0.88 (t, 3H, $\text{N-CH}_2-(\text{CH}_2)_{10}$ -

CH₃), 1.2-1.9 (br, 20H, N-CH₂-(CH₂)₁₀-CH₃), 2.4-4.2 (br, 6H, N-CH₂-(CH₂)₁₀-CH₃ and -NCH₂CH₂-), 7.20 (s, 2H, *ortho*-Ar), 7.27 (s, 1H, *para*-Ar), 7.48 (s, 2H, *meta*-Ar).

As shown in Scheme 2.1C, 2.0 g of **3** was dissolved in 40 mL of CH₂Cl₂ and stirred with 40 mL of CF₃COOH for 1 h at room temperature, followed by adding 40 mL of CH₃OH and stirring for an additional 30 min (15, 17, 18). The volatiles were removed under vacuum, and 100 mL of a neutralizing solution (0.5% (w/v) tetraethylammonium bromide and 5% (v/v) pyridine in CHCl₃) was added and stirred for 15 min. This solution was dialyzed twice against 2 L of the neutralizing solution for 12 h and then thrice against 2 L of CHCl₃ for 12 h. The yield of deprotected *N*-dodecyl-PEI (**4**) was 1.6 g. ¹H NMR (500 MHz, CD₂Cl₂, δ): 0.88 (t, 3H, N-CH₂-(CH₂)₁₀-CH₃), 1.2-1.9 (br, 20H, N-CH₂-(CH₂)₁₀-CH₃), 2.4-4.2 (br, 6H, N-CH₂-(CH₂)₁₀-CH₃ and -NCH₂CH₂-).

As shown in Scheme 2.1D, 0.75 g of **4** in 5 mL of anhydrous CH₂Cl₂ was stirred with 8.8 μL of *N,N*-diisopropylethylamine for 5 min and then combined with 5 mL of 1% (w/v) *N*-succinimidyl-6-(4'-azido-2'-nitrophenylamino)hexanoate (SANPAH) (Thermo Scientific) in anhydrous CH₂Cl₂. This mixture was stirred at room temperature in the dark for 1 h before dialysis against 1 L of CH₂Cl₂ for 14 h, after which time the solvent was removed under vacuum. The yield of *N,N*-ANPAH,dodecyl-PEI (**5**), where ANPAH is 6-(4'-azido-2'-nitrophenylamino)hexanoyl), was 0.73 g. ¹H NMR (500 MHz, CD₂Cl₂, δ): 0.88 (t, 3H, N-CH₂-(CH₂)₁₀-CH₃), 1.2-1.9 (br, 20H, N-CH₂-(CH₂)₁₀-CH₃), 2.4-4.2 (br, 6H, N-CH₂-(CH₂)₁₀-CH₃ and -NCH₂CH₂-), 6.8-7.9 (3H, ArN₃).

As shown in Scheme 2.1E, 0.73 g of **5** was dissolved in 15 mL of anhydrous CH₂Cl₂ and stirred with 2 mL of CH₃I at 37°C in the dark for 24 h (6, 16). The volatiles were removed under vacuum. The yield of *N,N,N*-ANPAH,dodecyl,methyl-PEI (**6**) was 0.83 g (the physical

appearance of the polymer is shown in Figure 2.1A). ^1H NMR (500 MHz, CD_2Cl_2 , δ): 0.88 (t, 3H, $\text{N-CH}_2\text{-(CH}_2\text{)}_{10}\text{-CH}_3$), 1.2-1.9 (br, 20H, $\text{N-CH}_2\text{-(CH}_2\text{)}_{10}\text{-CH}_3$), 2.4-4.2 (br, 9H, $\text{N-CH}_2\text{-(CH}_2\text{)}_{10}\text{-CH}_3$, N-CH_3 and $\text{-NCH}_2\text{CH}_2\text{-}$), 6.8-7.9 (3H, ArN_3).

Covalent modification of cotton

Woven undyed cotton sheets (ITW TexWipe) were cut into 2.5 x 2.5 cm pieces, ultrasonicated in isopropyl alcohol for 5 min, dried at 80°C , and autoclaved (Fig. 2.1C).

For photocopying, the cotton pieces were dipped in a 50 mg/mL solution of **6** in CH_2Cl_2 (Fig. 2.1B) for 1 min, allowed to dry in darkness, and irradiated on both sides at 365 nm with an 8-watt hand-held UV lamp (UVP EL series) at a 1-cm distance for 30 min. The resultant pieces of cotton were washed in CH_2Cl_2 , allowed to dry, and then the same procedure was repeated twice more. To maximize the removal of the unbound polymer, the **6**-photocopyed cotton was washed further. The resultant cotton sample gained a yellowish tint (Fig. 2.1D).

Covalent immobilization of *N,N*-hexyl,methyl-PEI to cotton was performed as described previously (3).

Surface characterization

The surface elemental analysis of plain cotton and **6**-photocopyed cotton by XPS was performed on a Kratos HS-AXIS spectrometer with an Al anode by Arkema, Inc.

The quaternary ammonium groups were quantified as previously described (3). Briefly, 1 cm^2 samples of plain and **6**-photocopyed cotton were shaken in 1 mL of 1% aqueous fluorescein solution for 5 min before shaking twice with 50 mL of water for 10 min at 250 rpm. The surface-bound fluorescein was displaced with 0.9 mL of 0.25% cetyltrimethylammonium

chloride at 250 rpm for 10 min. After addition of 0.1 mL of 0.1 M phosphate buffer (pH 8.0) to the detergent solution, the absorbance was measured at 501 nm; the previously determined (5) extinction coefficient of $77,000 \text{ M}^{-1} \text{ cm}^{-1}$ was used for quantification.

Waterborne bactericidal assay

E. coli (the Coli Genetic Stock Center, CGSC4401) and *S. aureus* (ATCC 33807) were cultured and prepared as previously described (16).

Bactericidal efficiency was determined using 2.5 x 2.5 cm pieces of cotton immersed in, and shaken with, 10 mL of a 4×10^4 cells/mL bacterial suspension in phosphate-buffered saline (PBS) at 250 rpm. Incubations with *E. coli* and *S. aureus* were performed at 37°C for 2 h and at room temperature for 4 h, respectively. Assays with plain and 6-photocoated cotton were used to determine their respective effects on bacterial viability, while otherwise identical conditions without cotton determined the initial bacterial viability. Of these, 5-fold serial dilutions were plated onto yeast-dextrose broth (YDB) agar plates and grown overnight at 37°C.

Viability of bacteria adhered to plain cotton, to *N,N*-hexyl,methyl-PEI derivatized cotton (included herein as a positive control), and to 6-photocoated cotton was determined immediately post-assay. Cotton samples tested against *S. aureus* were briefly dipped thrice in 40 mL of PBS to displace any non-adhered cells (4) and incubated with 20 mL of YDB at 250 rpm and 37°C. At 0.5-h intervals, these suspensions were briefly vortexed and 100- μ L aliquots were plated onto YDB-agar plates and grown overnight at 37°C.

2.5 References

1. Klibanov AM (2007) Permanently microbicidal materials coatings. *J Mater Chem* 17:2479-2482.
2. Goddard JM, Hotchkiss JH (2007) Polymer surface modification for the attachment of bioactive compounds. *Prog Polym Sci* 32:698-725.
3. Lin J, Qiu SY, Lewis K, Klibanov AM (2003) Mechanism of bactericidal and fungicidal activities of textiles covalently modified with alkylated polyethylenimine. *Biotechnol Bioeng* 83:168-172.
4. Tiller JC, Lee SB, Lewis K, Klibanov AM (2002) Polymer surfaces derivatized with poly(vinyl-*N*-hexylpyridinium) kill airborne and waterborne bacteria. *Biotechnol Bioeng* 79:465-471.
5. Tiller JC, Liao CJ, Lewis K, Klibanov AM (2001) Designing surfaces that kill bacteria on contact. *Proc Natl Acad Sci USA* 98:5981-5985.
6. Park D, Wang J, Klibanov AM (2006) One-step, painting-like coating procedures to make surfaces highly and permanently bactericidal. *Biotechnol Prog* 22:584-589.
7. Mukherjee K, Rivera JJ, Klibanov AM (2008) Practical aspects of hydrophobic polycationic bactericidal "paints". *Appl Biochem Biotechnol* 151:61-70.
8. Dick CR, Ham GE (1970) Characterization of polyethylenimine. *J Macromol Sci Chem* A-4:1301-1314.
9. Lin J, Qiu SY, Lewis K, Klibanov AM (2002) Bactericidal properties of flat surfaces and nanoparticles derivatized with alkylated polyethylenimines. *Biotechnol Prog* 18:1082-1086.
10. Scriven EFV ed (1984) *Azides and Nitrenes: Reactivity and Utility* (Academic Press, Orlando).
11. Krakowiak KE, Bradshaw JS (1998) Selective protection of the primary amine functions of linear tetraamines using the trityl group. *Synth Commun* 28:3451-3459.
12. Lyon B (2010) ITW Texwipe, productions manager.
13. Despotopoulou M (2010) Arekema Inc., materials analysis manager.
14. Milovic NM, Wang J, Lewis K, Klibanov AM (2005) Immobilized *N*-alkylated polyethylenimine avidly kills bacteria by rupturing cell membranes with no resistance developed. *Biotechnol Bioeng* 90:715-722.
15. Wuts PGM, Greene TW (2007) *Greene's Protective Groups in Organic Synthesis* (Wiley, Hoboken) 4th Ed.
16. Haldar J, Weight AK, Klibanov AM (2007) Preparation, application and testing of permanent antibacterial and antiviral coatings. *Nature Protoc* 2:2412-2417.
17. Canle M, Demirtas I, Maskill H (2001) Substituent effects upon rates of deamination and base strengths of substituted *N*-tritylamines. *J Chem Soc Perkin Trans 2*:1748-1752.
18. Theodorou V, Ragoussis V, Strongilos A, Zelepos E, Eleftheriou A, Dimitriou M (2005) A convenient method for the preparation of primary amines using tritylamine. *Tetrahedron Lett* 46:1357-1360.

Chapter 3. On structural damage incurred by bacteria upon exposure to hydrophobic polycationic coatings

3.1 Introduction

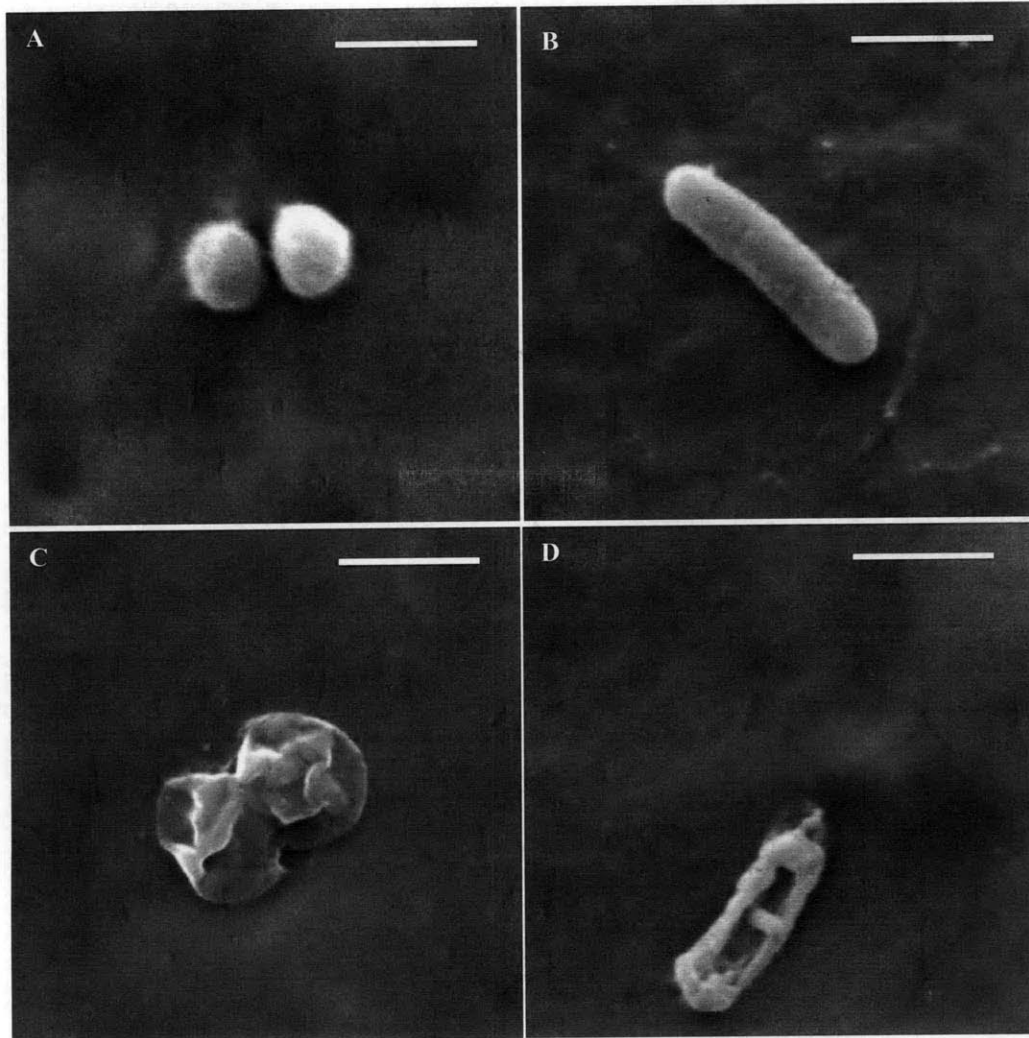
Further innovation in this area would benefit from understanding the mechanism by which our coatings inactivate microbes. We have previously demonstrated that upon exposure to certain *N*-alkylated-PEIs (PEI = polyethylenimine) both Gram-negative and Gram-positive bacteria are killed because the integrity of their cellular membranes is compromised (1, 2). Herein we report further progress in elucidating how these hydrophobic polycations kill bacteria. In particular, we have determined by scanning electron microscopy (SEM) that bacteria suffer severe structural damage upon contact with the *N,N*-dodecyl,methyl-PEI surface coatings. This damage, in turn, results in the leakage of significant quantities of proteins disproportionately from the periplasmic, as opposed to cytoplasmic, cellular space. Side-by-side comparison of these observations with those upon traditional lysozyme treatment in the presence of the chelating agent EDTA reveals striking similarities.

3.2 Results and Discussion

Our previous bactericidal studies have demonstrated that both waterborne and airborne bacteria are killed upon contact with either covalently attached *N,N*-hexyl,methyl-PEI or physically deposited *N,N*-dodecyl,methyl-PEI (2, 3). These observations, however, provided only limited insights into *how* bacteria were killed. In particular, a fluorescent assay that assessed viability of bacteria by their ability to accumulate a membrane-impermeable dye not only confirmed the potent bactericidal action results independently but also indicated that the integrity of the bacterial membrane was compromised by the hydrophobic polycations (1, 2).

To elucidate the magnitude of the imparted damage, we used scanning electron microscopy (SEM) to visually characterize the morphology of bacteria upon contact with microbicidally painted surfaces. The micrographs presented in Figures 3.1A and 3.1B for *S. aureus* and *E. coli*, respectively, on a bare silicon wafer show that they retain a well-defined morphology and surface smoothness characteristic of unperturbed bacteria, as previously demonstrated (4). In contrast, after contact with *N,N*-dodecyl,methyl-PEI-coated Si, both *S. aureus* and *E. coli* (Figs. 3.1C and 3.1D, respectively) exhibit profound morphological deformations. The shrunken appearance of these impacted bacteria indicates a loss of structural integrity, which is predominately maintained by the cellular wall (5), thereby suggesting a specific and undermining interaction with the bacteria's peptidoglycan layer by the hydrophobic polycations. While these SEM images allow us to visually confirm the damage to the bacteria, its specific details remained obscure. To illuminate them, we examined the solution for leaked intracellular proteins and compared the findings with those obtained upon the destruction of bacterial cells using standard microbiological lysis techniques.

Figure 3.1. Scanning electron microscopy images of *S. aureus* and *E. coli* K12 in contact with bare silicon wafers (**a** and **b**, respectively) and with those coated with *N,N*-dodecyl,methyl-PEI (**c** and **d**, respectively). The SEM micrographs shown are representative for their respective bacterial conditions; the scale bars equal 1 μm .



To this end, we first incubated *E. coli* K12 suspensions in plain and *N,N*-dodecyl,methyl-PEI-coated polypropylene tubes and monitored both their bacterial viability and protein leakage over time. As seen in Figure 3.2, incubation of *E. coli* in bare tubes gives rise to small amounts of protein in solution over 6 h, which can be attributed to secreted extracellular proteins (6). However, when the bacterial cells were incubated in the bactericide- painted tubes under the same conditions, a dramatic increase (e.g., 170% after 6 h) in protein concentration over these baseline levels was observed (Fig. 3.2). In parallel with the protein leakage, the bactericidal efficiency also rises with time of incubation (to reach $99 \pm 1\%$ after 6 h, see Fig. 3.2). Therefore, in addition to the bacterial membranes being permeabilized enough for small-molecule dyes to move across the membrane (1, 2), the degree of the damage inflicted by the hydrophobic polycations is so extensive that even intracellular proteins can escape into solution.

The generality of these findings was confirmed when we similarly tested the drug-resistant *E. coli* BAA-196, as well as *S. aureus*, and found 300% and 160%, respectively, more protein in solution compared with the bare polypropylene tube experiments (the first two lines in Table 3.1).

To calibrate the protein released upon incubation in a polycation-coated tube, we separately subjected *E. coli* K12 to a traditional lysozyme/EDTA treatment, which is known to permeate the outer membrane due to the presence of the chelator EDTA, and to enzymatically degrade the cell wall, shedding the cell's periplasmic constituents (7). As seen in Table 3.1, there is a 140% increase in protein concentration over the baseline, i.e., similar to that seen with the polycation treatment.

Figure 3.2. The effect of the *N,N*-dodecyl,methyl-PEI coating on the viability of *E. coli* K12 and on the bacterial protein concentration released into solution (see text for details). The shaded bars represent bactericidal efficiencies; error bars were omitted for clarity. Total protein in solution after incubation with plain (\square) and *N,N*-dodecyl,methyl-PEI-coated (\blacksquare) polypropylene tubes are shown by lines. All values were obtained in duplicate, and are shown as averages \pm standard deviations

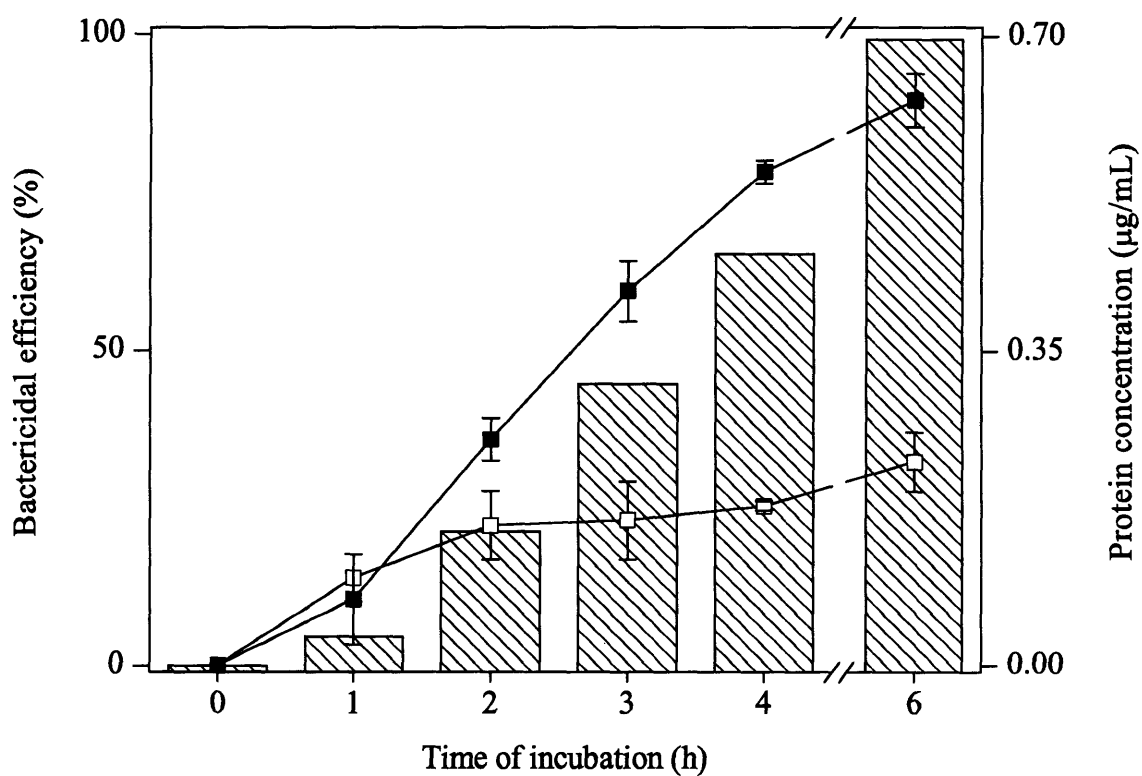


Table 3.1. The protein concentrations released into solution by *E. coli* and *S. aureus* after various treatments. Each measurement was performed in duplicate, and the values are given as averages \pm standard deviations

Treatment	Total protein concentrations ($\mu\text{g/mL}$)		
	<i>E. coli</i> K12	<i>E. coli</i> BAA-196 ^a	<i>S. aureus</i>
None	0.23 \pm 0.03	0.23 \pm 0.03	0.20 \pm 0.04
<i>N,N</i> -Dodecyl,methyl-PEI coating	0.63 \pm 0.03	0.93 \pm 0.01	0.53 \pm 0.01
Lysozyme/EDTA	0.56 \pm 0.05		
French press	15.6 \pm 0.6	14.8 \pm 0.7	3.2 \pm 0.3

^aThe same conditions as with the K12 strain.

To put the quantity of the leaked protein into perspective vis-à-vis the total amount of protein in the cell, we separately employed the French press treatment commonly used for extensive cell lysis (8, 9). One can see in Table 3.1 that for the three tested kinds of bacteria, there is far more protein generated by the French press disintegration than released by polycation or lysozyme/EDTA treatments. Specifically, after correction for the baseline extracellular proteins, the 6-h exposure to *N,N*-dodecyl,methyl-PEI coatings yields 2.6%, 4.6%, and 2.1% of the proteins extracted in the French press treatment for *E. coli* K12, *E. coli* BAA-196, and *S. aureus*, respectively (Table 1). That these amounts, however, are comparable with those produced in the lysozyme/EDTA treatment (2.1% for *E. coli* K12) suggests that mechanistically these two dissimilar modes of lysis may nevertheless target the same bacterial components.

Since the lysozyme/EDTA treatment is known to release the periplasmic proteins and leave the cytoplasm relatively intact (7), we focused on determining the origins of the leaked proteins resulting from exposure to the *N,N*-dodecyl,methyl-PEI coating. To this end, we measured the concentrations of the β -lactamase and β -galactosidase enzymes leaked into solution from *E. coli* as indicators of the polycationic chain's penetration into the periplasm and cytoplasm, respectively.

Table 3.2. The concentrations of periplasmic and cytoplasmic enzymes (β -lactamase and β -galactosidase, respectively) released into solution by *E. coli* after various treatments. Each measurement was performed in duplicate, and the values are given as averages \pm standard deviations

Treatment	<i>E. coli</i> enzyme concentrations (ng/mL)	
	β -Lactamase ^a	β -Galactosidase ^a
None	0.060 \pm 0.001	1.9 \pm 0.2
<i>N,N</i> -Dodecyl,methyl-PEI coating	0.11 \pm 0.01	9.9 \pm 0.6
French press	0.68 \pm 0.04	1700 \pm 100

^a Since *E. coli* K12 did not produce measurable levels of β -lactamase, *E. coli* BAA-196 was employed to assay for leakage of β -lactamase, while the former strain to assay for leakage of β -galactosidase.

As seen in Table 3.2, upon contact with the hydrophobic polycation *E. coli* gave 83% and 420% above the baseline quantities of β -lactamase and β -galactosidase, respectively. Normalization to the total proteins yielded by French press shows that for *E. coli* 8.1% of β -lactamase is leaked from the cells, as compared to 4.6% of the total protein, or a disproportionately large fraction of this periplasmic enzyme (Table 3.2). With respect to β -galactosidase, 0.5% of it is leaked from *E. coli*, as compared to 2.6% of the total protein, or a disproportionately small fraction of the cytoplasmic enzyme (Table 3.2). Taken together these results indicate that relatively larger quantities of periplasmic proteins are leaked when compared to cytoplasmic ones, which suggests that the periplasm is breached by the polycationic chains significantly more than the cytoplasm. In other words, there appears to be considerable damage to the outer membrane and relatively minor damage to the cytoplasmic membrane. Since both the quantity of proteins leaked and the nature of the damage by the *N,N*-dodecyl,methyl-PEI coating are very similar to those imparted by a traditional lysozyme/EDTA treatment, the two treatments may target the same bacterial structures, namely the outer membrane and the peptidoglycan cell wall.

3.3 Conclusion

Herein we report that upon exposure to the hydrophobic polycationic coating (*N,N*-dodecyl,methyl-PEI), substantial damage is imparted to *S. aureus* and *E. coli* (Gram-positive and Gram-negative bacteria, respectively) as revealed by SEM. Further investigation into this phenomenon shows an increasing protein leakage over time, corresponding with an increasing bactericidal activity. Of the proteins released, we discovered a disproportionately large fraction of β -lactamase enzyme and a disproportionately small fraction of β -galactosidase leaked into solution as compared their nominal cellular concentrations. This indicates substantially more damage was done to the outer membrane than the cytoplasmic membrane. In addition, there were striking similarities in overall bacterial leakage upon exposure to the polycationic coating with lysozyme/EDTA treatment, supporting our hypothesis that there is considerably damage imparted to the cell wall.

3.4 Materials and Methods

Materials

All chemicals, unless otherwise noted, were obtained from Sigma-Aldrich Chemical Co. Silicon (Si) wafers were from Silicon Quest International.

Linear PEI was synthesized as previously described (10). Briefly, 20 g of poly(2-ethyl-2-oxazoline) ($M_w = 500$ kDa) was refluxed in 800 mL of 24% (v/v) HCl at 125°C for 96 h. The formed precipitate was filtered off, dissolved in water, and neutralized with excess KOH until re-precipitation. Following filtration and washing with water to a neutral pH, the precipitate was dried under vacuum to give 7.6 g of 217-kDa linear PEI.

Synthesis of *N,N*-dodecyl,methyl-PEI was performed similarly to a previously described method (11). Briefly, a mixture of 4.0 g of linear PEI, 15.4 g of KOH, 60 mL of 1-bromododecane, and 50 mL of *tert*-amyl alcohol was stirred at 95°C for 96 h, after which the solids were removed by centrifugation at 6,000 rpm for 30 min at room temperature. The supernatant was stirred with 15 mL of iodomethane in a sealed flask at 60°C for 24 h. The resulting polymer was extracted by precipitation with an excess of ethyl acetate, followed by filtering and drying under vacuum. The yield was 12.2 g.

N,N-Dodecyl,methyl-PEI coatings were prepared by painting the surfaces with a 50 mg/mL polycation solution in chloroform with a 3/8 inch nylon-bristled paint brush (Loew-Cornell) and then allowing the solvent to evaporate. Coating and drying was performed in quadruplicate.

Scanning electron microscopy

Staphylococcus aureus (*S. aureus*) (ATCC, 33807) was grown overnight at 37°C in cation-adjusted Mueller Hinton Broth II (CMHB) (Difco, BD), washed, and prepared as previously described (12), then diluted to 5×10^6 cells/mL and sprayed onto surfaces using a chromatography sprayer (VWR International) at ~10 mL/min. Preparation and spraying of *Escherichia coli* (*E. coli*) K12 (the Coli Genetic Stock Center, CGSC4401) was performed similarly, except that it was cultured in LB-Miller broth (VWR) and diluted to 5×10^7 cells/mL.

Sprayed samples of both plain and *N,N*-dodecyl,methyl-PEI-coated Si wafers were incubated at room temperature for 30 min, and then fixed using the Karnovsky's Fixative kit (Polysciences) according to manufacturer's instructions. Briefly, samples were incubated in a fixing solution (2% paraformaldehyde plus 2.5% glutaraldehyde in 0.1 M Na phosphate buffer, pH 7.4) for 2 h and rinsed for 10 min in phosphate buffer. They were then incubated in 1% osmium tetroxide solution for 1 h in darkness, rinsed with the phosphate buffer, and serially dehydrated in 35%, 50%, 70%, and 95% ethanol solutions for 10 min each, before final dehydration (repeated thrice) in pure anhydrous ethanol for 10 min. Samples were then freeze-dried in liquid nitrogen and sputter-coated before imaging with a JEOL JSM-6060 scanning electron microscope at a 11,000X magnification.

Bacterial lysis

E. coli K12 and *S. aureus* were cultured and prepared as described previously (12). Multi-drug-resistant, extended-spectrum β -lactamase *E. coli* (ATCC, BAA-196) was grown overnight in tryptic soy medium (BD) with 10 μ g/mL ceftazidime (Sigma-Aldrich) at 37°C (12).

Lysozyme treatment of bacterial cells, based on previously described procedures (13), comprised incubating 10^8 cells/mL of *E. coli* K12 in phosphate-buffered saline (PBS), 20% (w/v)

sucrose, 1 $\mu\text{g}/\text{mL}$ hen egg-white lysozyme (Sigma-Aldrich, $\sim 50,000$ units of activity per mg), and 10 mM EDTA (ethylenediaminetetraacetic acid Na salt) at 4°C for 2 h. French press treatment consisted of two passes at 16,000 psi using a French pressure cell press (Spectronic Instruments).

Exposure to surfaces painted by *N,N*-dodecyl,methyl-PEI consisted of shaking 10^8 cells/mL bacteria in polypropylene conical centrifuge tubes at 250 rpm. For *E. coli*, 40 mL of bacterial suspension was incubated in 50-mL tubes (BD), with an inner surface area of 94 cm^2 , for 6 h at 37°C . For *S. aureus*, 30 mL of bacterial suspension was incubated in a 50-mL tube with another 13-mL culture tube (BD) inserted in it (with an inner surface area of 143 cm^2) for 8 h at room temperature. Bacterial viability was assessed by plating serial dilutions of the bacterial suspension onto yeast-dextrose broth (YDB)-agar plates and incubating overnight at 37°C . The bactericidal efficiency was calculated by comparing the numbers of colony-forming units (CFU) of suspensions incubated in plain tubes with those in the case of *N,N*-dodecyl,methyl-PEI-coated tubes.

Protein purification and enzymatic assays

Protein extracts from the aforementioned treatments were obtained by centrifugation of the treated bacterial suspensions at 4,000 rpm at 4°C for 10 min and subsequent concentration of the supernatant to 1.5 mL using Amicon Ultracel 3k Centrifugal Filters (Millipore). The resultant solutions were analyzed with a standard BSA Bradford assay or further concentrated to 0.1 mL using Amicon Ultracel 10k Centrifugal Filters (Millipore) for β -lactamase and β -galactosidase assays.

The β -lactamase assay was executed using the chromogenic reagent Nitrocefin (EMD Chemicals) according to manufacturer's instructions. A mixture of 100 μ L each of a concentrated sample and of 50 μ g/mL Nitrocefin in PBS was incubated at 37°C for 10 min, and the change in absorbance was measured at 486 nm. Sample solutions were referenced to standard curves constructed from purified *Enterobacter cloacae* β -lactamase (Sigma-Aldrich) in PBS.

The β -galactosidase assay employed the β -Gal Assay Kit (Invitrogen) according to manufacturer's instructions. After combining 30 μ L of a concentrated sample with 70 μ L of 4 mg/mL *ortho*-nitrophenyl- β -galactoside (ONPG) and 200 μ L of phosphate buffer, pH 7.0, supplemented with KCl, MgSO₄, and β -mercaptoethanol at 37°C for 30 min, the reaction was stopped with 500 μ L of 1 M Na₂CO₃. The absorbance measured at 420 nm was referenced to standard curves based on purified *E. coli* β -galactosidase (Sigma-Aldrich) in PBS.

3.5 References

1. Milovic NM, Wang J, Lewis K, Klivanov AM (2005) Immobilized *N*-alkylated polyethylenimine avidly kills bacteria by rupturing cell membranes with no resistance developed. *Biotechnol Bioeng* 90:715-722.
2. Park D, Wang J, Klivanov AM (2006) One-step, painting-like coating procedures to make surfaces highly and permanently bactericidal. *Biotechnol Prog* 22:584-589.
3. Lin J, Qiu SY, Lewis K, Klivanov AM (2002) Bactericidal properties of flat surfaces and nanoparticles derivatized with alkylated polyethylenimines. *Biotechnol Prog* 18:1082-1086.
4. Belaouaj AA, Kim KS, Shapiro SD (2000) Degradation of outer membrane protein A in *Escherichia coli* killing by neutrophil elastase. *Science* 289:1185-1187.
5. Vollmer W, Blanot D, de Pedro MA (2008) Peptidoglycan structure and architecture. *FEMS Microbiol Rev* 32:149-167.
6. Glenn AR (1976) Production of extracellular proteins by bacteria. *Annu Rev Microbiol* 30:41-62.
7. Malamy MH, Horecker BL (1964) Release of alkaline phosphatase from cells of *Escherichia coli* upon lysozyme spheroplast formation. *Biochemistry* 3:1889-1893.
8. Jorgensen L, Oneill BK, Thomas CJ, Morona R, Middelberg APJ (1995) Release of chloramphenicol acetyl transferase from recombinant *Escherichia coli* by sonication and the French press. *Biotechnol Tech* 9:477-480.
9. Schmitt B (1976) Pyruvate dehydrogenase in *Escherichia coli*-an active 17S species in crude extracts. *Biochimie* 58:1405-1407.
10. Thomas M, Lu JJ, Ge Q, Zhang CC, Chen JZ, Klivanov AM (2005) Full deacylation of polyethylenimine dramatically boosts its gene delivery efficiency and specificity to mouse lung. *Proc Natl Acad Sci USA* 102:5679-5684.
11. Haldar J, An DQ, de Cienfuegos LA, Chen JZ, Klivanov AM (2006) Polymeric coatings that inactivate both influenza virus and pathogenic bacteria. *Proc Natl Acad Sci USA* 103:17667-17671.
12. Haldar J, Weight AK, Klivanov AM (2007) Preparation, application and testing of permanent antibacterial and antiviral coatings. *Nature Protoc* 2:2412-2417.
13. Yamato I, Anraku Y, Hirosawa K (1975) Cytoplasmic membrane vesicles of *Escherichia coli*: I. A simple method for preparing the cytoplasmic and outer membranes. *J Biochem* 77:705-718.

Chapter 4. On the mechanism of inactivation of influenza viruses by immobilized hydrophobic polycations

4.1 Introduction

Infectious diseases, including influenza, kill millions of people a year and sicken hundreds of millions (1, 2). In the United States alone, there are tens of thousands of influenza-related deaths annually (3). The influenza virus' propensity for genomic recombination and mutation (antigenic shift and drift, respectively) can generate new strains to which humans have no previously developed immunity — a common factor in influenza pandemics (4, 5). A jarring example in modern history is the Spanish Flu of 1918-1919, which killed up to 100 million people worldwide (6); the H1N1 (“Swine Flu”) virus of 2009 has shown such pandemics to remain an acute threat. Although vaccines and such antivirals as zanamivir and oseltamivir (Relenza[®] and Tamiflu[®], respectively) are somewhat effective, they have serious limitations: the former must predict the next seasonal flu strain months in advance for current egg-based vaccines (7), while the latter are unreliable because of rapid mutations in the influenza virus epitopes (8).

A complementary approach to vaccines and drugs is to inactivate the virus (or any pathogenic microbe) with biocides during its transmission through inanimate objects, which is a major route for nosocomial infections (9, 10). However, biocidal formulations commonly applied as solutions can evaporate, be used up, or wiped away, making the efficacy of this approach dependent on the frequency of its reapplication.

We have demonstrated (11) that coating (“painting”) with polyethylenimine (PEI)-based hydrophobic polycations renders surfaces permanently antibacterial and antifungal, retaining

their disinfectant properties even after multiple washes (12, 13). Recently, this antimicrobial activity has been expanded to influenza viruses (14, 15). Herein we report a mechanistic elucidation of this phenomenon. Specifically, we have found that upon contact with *N,N*-dodecyl,methyl-PEI coatings, aqueous solutions of influenza A viruses (including human and avian, both wild-type and mutant zanamivir-resistant, strains) are completely disinfected; this correlates with a disappearance of viral proteins, although significant quantities of viral RNA are still in solution. Based on this evidence, we conclude that these solutions are disinfected by the removal of viral particles that irreversibly adhere to the hydrophobic polycationic coatings; the latter then cause disintegration (including RNA release) and inactivation of the adhered viruses.

4.2 Results and Discussion

Prior to embarking on a mechanistic investigation of virucidal properties of surfaces coated (“painted”) with *N,N*-dodecyl,methyl-PEI, we explored whether the nature of the underlying solid surface plays a role. To this end, since the virucidal activity of these hydrophobic polycations was previously discovered with coated glass slides (14, 15), we now added to these studies chemically unrelated polyethylene and polypropylene surfaces. As seen in Table 4.1, bare (i.e., uncoated) slides of each material exhibited only partial or no virucidal activity against a waterborne influenza virus (WSN strain). In contrast, when coated with *N,N*-dodecyl,methyl-PEI, all three types of surfaces completely disinfected the aqueous solutions of the virus, indicating that this property is independent of the solid surface treated.

Next, we asked what happens to the virus when the solution is disinfected. While quantifying the influenza virus by the plaque assay (16) allowed us to titer the infectivity of solution, the fate of the viral particles remained obscure. In particular, we could not discriminate between the following possibilities: (i) the viruses collide with the coated surface, undergo irreversible inactivation, and bounce off back into solution, or (ii) the viruses collide with the coated surface and irreversibly adhere to it in either an infectious or non-infectious form. To distinguish between these alternative scenarios, we employed the viral nucleoprotein (NP), which is one of the more prevalent influenza proteins (some 1000 copies/viron) (4), as a marker for the viral particles. Note that although NP is an internal viral protein, it can be easily quantified following lysis of viral particles.

Table 4.1. The effect of glass, polypropylene, and polyethylene slides coated with *N,N*-dodecyl,methyl-PEI on WSN influenza strain's viral infectivity and concentration of viral particles in solution.

Surface	Infectivity (by plaque assay)*			Viral particles (by ELISA)*,†		
	Initially	After contact	After contact with	Initially	After contact	After contact with
		with bare slides	polycation-coated slides		with bare slides	polycation-coated slides
Glass	20.4 ± 2.1	10.9 ± 0.5	0.0 ± 0.0	21.0 ± 2.2	1.4 ± 2.1	0.0 ± 1.6
Polypropylene	20.4 ± 2.1	18.1 ± 1.9	0.0 ± 0.0	21.0 ± 2.2	17.8 ± 1.1	-1.0 ± 2.2
Polyethylene	20.4 ± 2.1	15.1 ± 3.2	0.0 ± 0.0	21.0 ± 2.2	17.1 ± 1.2	0.1 ± 1.2

*Values represent titers: (mean ± std dev) x 10⁴ pfu/mL

†Assessed by measuring the concentration of viral nucleoprotein (NP); the high loss of viral particles for bare glass slides is likely due to non-specific adsorption of exogenous viral NP

The ELISA data for NP, i.e., viral particles, in aqueous solutions of an influenza virus (WSN strain) incubated between pairs of bare glass, polypropylene, or polyethylene slides revealed marked loss (presumably due to non-specific adsorption) of virions for glass but little for the two polymers (Table 4.1). When the slides were coated with *N,N*-dodecyl,methyl-PEI, however, the viral particles completely disappeared from solution regardless of what material was coated (Table 4.1). Therefore, all subsequent studies reported herein were performed with polyethylene slides because they displayed far less background adsorption than glass slides and were easier to work with than polypropylene slides.

To test the generality of the foregoing observations, our investigation was expanded to include other influenza viruses, namely a human pathogenic strain (PR8), as well as avian pathogenic wild-type (TurkWt) and mutant zanamivir-resistant (TurkMu) strains (Table 4.2). As can be seen in Figure 4.1A, virucidal activities of bare polyethylene slides are negligible against all of these strains. In contrast, the *N,N*-dodecyl,methyl-PEI-coated slides are completely virucidal (Fig. 4.1A), thus indicating that the hydrophobic polycationic coating is able to disinfect aqueous solutions of a variety of diverse influenza strains. Separately, the independent ELISA results depicted in Figure 4.1B show that while the bare slides had minor effect on viral particle concentrations, the viral particles disappeared from solution after incubation with the polycation-coated slides. Thus by using influenza's NP as a marker, we find a strong correlation between the disinfection of the viral solution and the disappearance of the viral particles from it. This observation suggests that the influenza viral particles adhere to the hydrophobic polycationic coatings. It is noteworthy that this adherence takes place regardless of variables arising from the source of culture, suspension media, and antigenicity associated with the different strains used (Table 4.2).

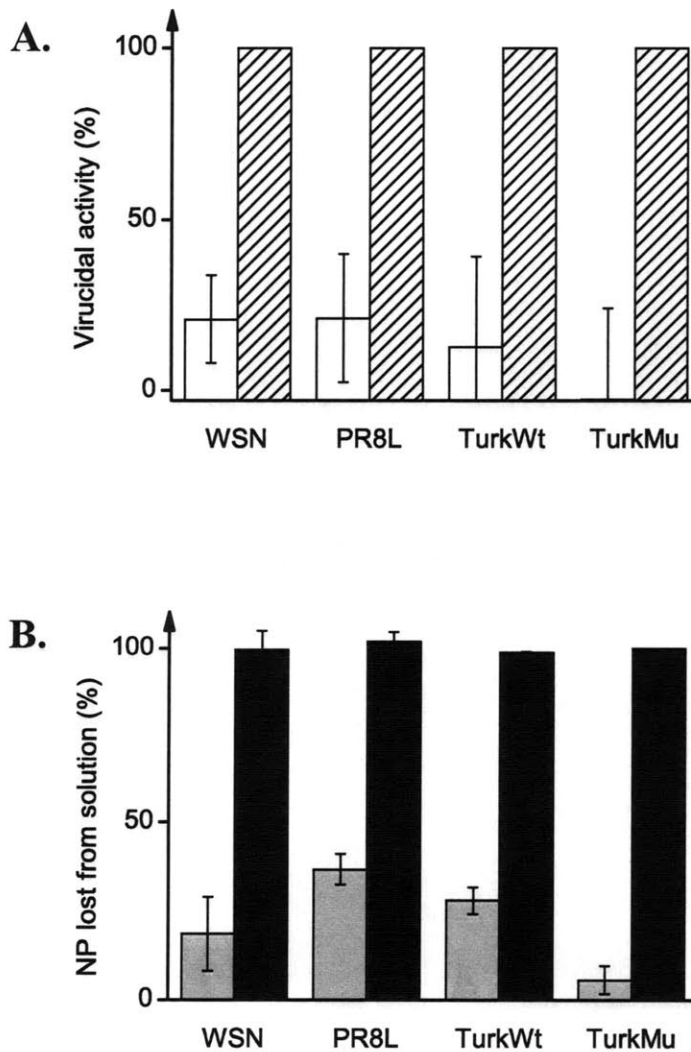
Table 4.2. Strains of influenza A viruses used in this study and their properties.

Short name	Influenza A viral strain	Initial titer (pfu/mL)*	Culture conditions; suspension conditions	Notes
WSN	WSN/33 (H1N1)	$4.5 (\pm 0.6) \times 10^6$	Tissue; DME-HEPES/10% FBS	Laboratory strain, non-pathogenic
PR8H	PR/8/34 (H1N1)	$1.3 (\pm 0.5) \times 10^8$	Egg; HEPES/saline	Human pathogenic; sucrose-gradient purified
PR8L [†]	PR/8/34 (H1N1)	$0.9 (\pm 0.2) \times 10^6$	Egg; HEPES/PBS/saline	Human pathogenic; sucrose-gradient purified
TurkWt	turkey/MN/833/80 (H4N2)	$1.0 (\pm 0.1) \times 10^6$	Egg; allantoic fluid	Avian pathogenic
TurkMu	turkey/MN/833/80 (H4N2)	$4.3 (\pm 0.3) \times 10^6$	Egg; allantoic fluid	Avian pathogenic; zanamivir-resistant

*Determined *via* plaque assay after ribonuclease pretreatment; the titer is that of a 10- μ L droplet incubated with slides prior to a 100-fold dilution upon washing. See Materials and Methods for details.

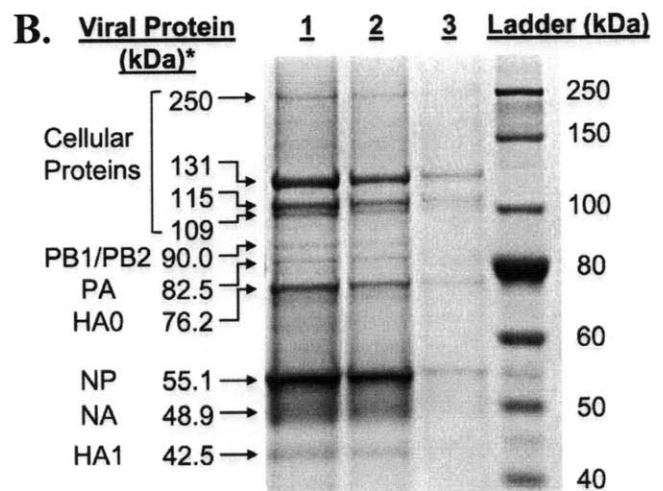
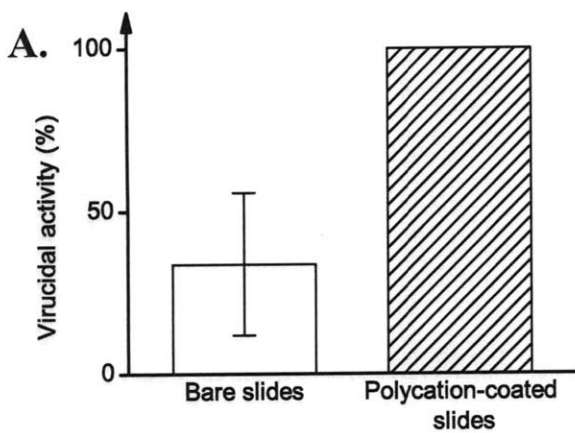
[†]An approximately 100-fold dilution of PR8H with PBS

Figure 4.1. The effect of polyethylene slides coated with *N,N*-dodecyl,methyl-PEI challenged with aqueous solutions of various influenza A viruses. See Table 2 for viral strain abbreviations and details (note that “H” and “L” after PR8 stand for high and low titer of the virus, respectively). (A) Virucidal activity of bare (□), and polycation-coated polyethylene slides (▨) against various influenza virus strains. (B) Relative quantities of viral nucleoprotein (NP) disappeared from solution after incubation with bare (□), and with polycation-coated polyethylene slides (■).

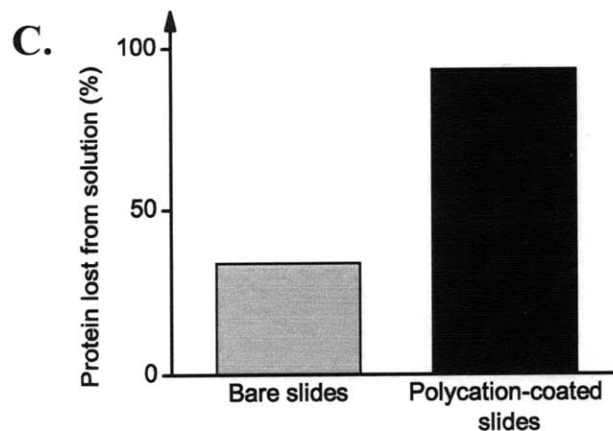


To independently verify these results and to test for other influenza viral proteins in solution, we examined *N,N*-dodecyl,methyl-PEI-coated slides against a solution of the purified PR8H virus (which differs from PR8L only by its much higher titer; Table 4.2) and confirmed its complete disinfection (Figure 4.2A). Additionally, we analyzed the initial viral solution, as well as that after exposure to either bare or polycation-coated slides, by means of SDS-PAGE. Even a visual inspection of protein band profiles in lanes 1, 2, and 3 in Figure 4.2B reveals some loss for each protein after the exposure, with by far the most dramatic one occurring with the virus incubated with the polycation-coated slides (lane 3 in Fig. 4.2B). Quantification of these observations by gel-scanning densitometry indicates a total loss of 94% of viral protein after incubation with the polycation-coated slides *versus* only a 34% loss after incubation with control bare slides (Fig. 4.2C). (That the bare slides demonstrated the same losses in virucidal activity (Fig. 4.2A) as in viral protein suggests a non-specific removal of the virus from solution.) The observed complete loss of virucidal activity *versus* a concurrent nearly complete loss of viral protein suggests that a small fraction of inactivated influenza virus and/or protein-containing fragments thereof remains in solution even following incubation with coated slides, likely due to the much higher viral titer required for SDS-PAGE used in these experiments.

Figure 4.2. The effect of polyethylene slides coated with *N,N*-dodecyl,methyl-PEI on high-titer human pathogenic PR8 influenza virus strain (PR8H, Table 4.2). (A) Virucidal activity of PR8H by bare (□), and *N,N*-dodecyl,methyl-PEI-coated polyethylene slides (▨). (B) SDS-PAGE of the concentrated PR8H strain run on a 7% polyacrylamide gel and stained with the commassie blue dye. Lanes 1, 2, and 3 represent virus samples prior to assay, after contact with bare slides, and after contact with polycation-coated slides, respectively. (C) Protein disappeared from solution by bare slides (□), and polycation-coated slides (■), as determined by gel scanning densitometry.

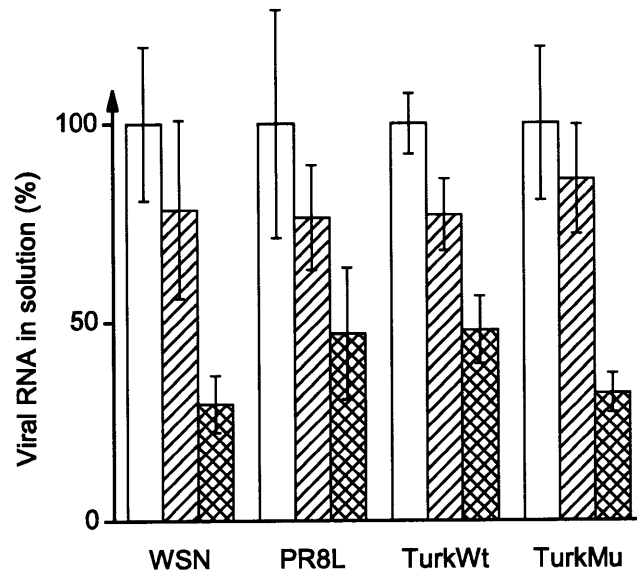


*Protein band assignments based on literature data (4, 35).



These findings support the second aforementioned scenario, namely that the viral particles irreversibly adhere to the *N,N*-dodecyl,methyl-PEI-coated surface, thereby vanishing from solution. To mechanistically explore this process further, we endeavored to assess the infectivity of the influenza viruses *adhered* to the coated surface. Since such viruses are not amenable to cell-based infectivity assays, we decided to examine instead how much viral RNA could be detected in solution. Its substantial presence there would evidence the inactivation of the surface-bound viruses because they obviously cannot be infective without their RNA. To this end, we used real-time reverse-transcriptase PCR (qRT-PCR) with the probe and primers detecting influenza virus's 7th RNA segment, i.e., the genomic region encoding the matrix (M₁) protein (4, 17). Using the same influenza strains (Table 4.2), negligible losses of viral RNA from solution were observed in the case of bare polyethylene slides (Figure 4.3). Importantly, and in sharp contrast to the results from our protein-based assays (Fig. 4.2), however, all viral solutions incubated with the *N,N*-dodecyl,methyl-PEI-coated slides exhibited significant quantities of viral RNA. This leakage of viral RNA from the surface-adhered viral particles points to a profound damage to the virus, inevitably leading to its demise.

Figure 4.3. Relative quantities of influenza A viral RNA in solution prior to assay (□), after incubation with bare polyethylene slides (▨), and after incubation with *N,N*-dodecyl,methyl-PEI-coated polyethylene slides (▩).



To ensure that the RNA detected in solution was indeed leaked from the interior of the viral particle, we pretreated all viral samples with the ribonuclease enzymes to digest any exogenous single- or double-stranded RNA that may be present (18-20). Control experiments confirmed that this enzymatic pretreatment completely digests RNA and that addition of ribonuclease's inhibitor prevents subsequent RNA digestion (see Appendix I). There was also no non-specific amplification from *N,N*-dodecyl,methyl-PEI putatively leached into solution (see Appendix I). A comparison of genomic sequences between influenza viral samples prior to, and after, contact with the polycationic coating revealed at least a 95% sequence identity (this less than a 100% identity is likely due to inherent errors in the sequencing technology (21)). All these results support the conclusion that the detected viral RNA is, in fact, endogenous viral genomic material leaked into solution after contact with the hydrophobic polycationic coating.

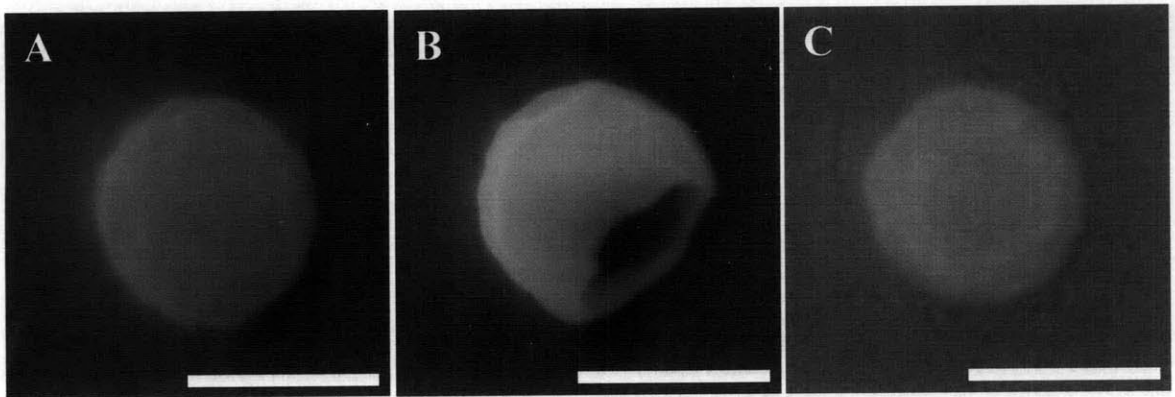
The recovery of RNA from the immobilized-*N,N*-dodecyl,methyl-PEI-contacted viral solutions was about half of that from the uncoated slides. This is in contrast to our protein studies which have thus far suggested an all-or-none virus inactivation scenario. Since the root of this partial recovery of genomic material may point to an additional mechanism in the polycation's virucidal activity, we directly visualized the viral particles on the surfaces using scanning electron microscopy (SEM). Micrographs of the WSN strain of influenza virus on a plain silicon wafer showed no visible damage to the former's structure (Figure 4.4A). In contrast, exposure of the viruses to the polycation-coated surface revealed a mixture of two extremes: either a substantial structural damage leaving a gaping hole (Fig. 4.4B) or no noticeable effect (Fig. 4.4C). Specifically, out of 132 exposed viral particles surveyed, most (54%) revealed the type of structural damage illustrated in Fig. 4.4B. Interestingly, this value is in agreement with the fraction of RNA recovered from the polycation-coated slides as compared to the bare slides

(Fig. 4.3). As to the observed (Figs. 4.4B and 4.4C) bimodal distribution, it is possible that even those viral particles that appear intact are actually damaged on the side facing the *N,N*-dodecyl,methyl-PEI coating and thus hidden from view; this type of damage would also likely hinder escape of viral RNA into solution.

One might have expected that no RNA should be recovered in solution at all due to non-specific electrostatic interactions between the negatively charged nucleic acid and the surface-situated hydrophobic polycation molecules if not for the fact that the derivatization of PEI with long alkyl moieties sterically interferes with such interactions (22-24). Note in this regard that elemental analysis of *N,N*-dodecyl,methyl-PEI used herein shows approximately 1.6 dodecyl moieties per monomer unit, corresponding to, on average, 60% of monomers in PEI doubly dodecylated and 40% singly dodecylated, which is considerably greater than in the previous reports (22-24).

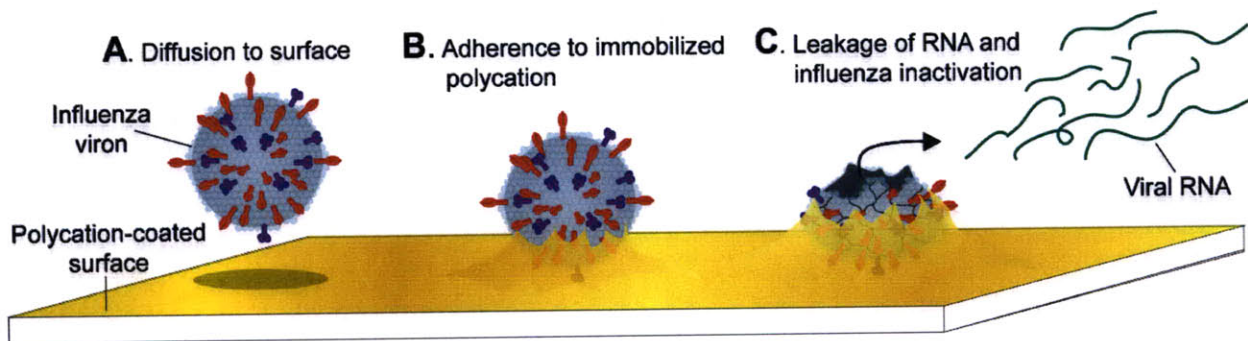
Finally, we addressed whether a monomeric structural analog of *N,N*-dodecyl,methyl-PEI, namely dodecyltrimethylammonium bromide (DTAB), was also capable of inactivating the influenza virus. To this end, we challenged the influenza virus with serial dilutions of DTAB for the latter's concentration required for 50% inhibition (IC_{50}) (25) (and also its toxic concentration, i.e., that reducing MDCK cell viability by 50%, TC_{50}). The DTAB's IC_{50} value was found to be 21 (± 5) $\mu\text{g/mL}$ (which was 4-fold lower than its measured TC_{50} value of 84 (± 26) $\mu\text{g/mL}$, in agreement with literature (26)). This finding suggests that the antiviral activity observed with our surface-immobilized hydrophobic polycations is inherent to the quaternary ammonium monomeric unit. Indeed, a similar quaternary ammonium salt, benzalkonium (alkylbenzyltrimethylammonium) chloride, is also capable of inactivating influenza virus (27-29).

Figure 4.4. Scanning electron microscopy (SEM) images of the WSN strain of influenza virus after exposure to plain (A), and *N,N*-dodecyl,methyl-PEI-coated (B and C) silicon wafers. Of the latter, a larger fraction of viral particles showed substantial structural damage (B), while a smaller fraction showed no visible damage (C); see text for details. Scale bars correspond to 100 nm.



Based on the experimental evidence obtained herein, we propose a framework for influenza virus inactivation depicted in Figure 4.5. It stipulates that when viral particles strike the polycation-coated surface due to thermal motion (Fig. 4.5A), they can adhere to it (Fig. 4.5B) through hydrophobic and electrostatic interactions (11). In this regard it is worth noting that, upon interactions with polycations, model lipid vesicles can undergo lateral segregation and flip-flopping (30) of phospholipids, ultimately fluidizing their membrane (31). These types of effects would disrupt the ordered lipid rafts (32, 33) and leaflet asymmetry (34) in influenza viral envelopes. Perhaps as a result of such interactions, a loss of virus's integrity ensues manifesting itself in a leakage of RNA into solution and a loss of infectivity (Fig. 4.5C).

Figure 4.5. Proposed mechanism of influenza A virus inactivation by *N,N*-dodecyl,methyl-PEI surface coatings. (A) An influenza viral particle diffuses to the polycation-coated surface from solution and (B) adheres to it. Significant damage imparted by the immobilized hydrophobic polycations is then incurred by the adhered viral particle such that (C) its genomic material (RNA) leaks into solution leaving the viral particle inactivated on the surface.



4.3 Conclusions

Through investigation into how aqueous solutions of various human and avian influenza viruses are disinfected by *N,N*-dodecyl,methyl-PEI coatings, we found that this phenomenon was dependent on neither the nature of the surface that was coated nor the strain of influenza A virus. A direct correlation was found between the exposed solution's losses of infectivity and of viral proteins, thereby indicating that the viral particles adhere to the surface-immobilized hydrophobic polycation. Additional analysis of the disinfected solution revealed significant quantities of RNA therein that stemmed from the viral particles, thereby evidencing that the integrity of the latter was compromised allowing the release of their genomic material. This conclusion was independently verified by direct SEM observations. A monomeric analog of *N,N*-dodecyl,methyl-PEI, DTAB, was also found to inactivate the influenza virus suggesting that the antiviral activity is inherent to the hydrophobic quaternary ammonium salt moiety, which is retained in even a polymeric and surface-immobilized form.

4.4 Materials and Methods

Polymer synthesis and immobilization

Unless otherwise noted, all chemicals were obtained from Sigma-Aldrich Chemical Co. Synthesis of *N,N*-dodecyl,methyl-PEI was performed as described previously (14, 16, 23). Briefly, linear PEI was obtained by acid hydrolysis of 20 g of poly(2-ethyl-2-oxazoline) (M_w of 500 kDa) in 800 mL of 24% (v/v) HCl solution under reflux at 125°C for 96 h. The precipitate was collected by vacuum filtration, dissolved in distilled water, re-precipitated at alkaline pH with excess KOH, and then filtered and washed with distilled water until reaching neutral pH. The product was lyophilized for 3 days to yield 7.6 g of 217-kDa linear PEI (23). A 4.0-g portion thereof was combined with 15.4 g of K_2CO_3 , 66 mL of 1-bromododecane, and 50 mL of *tert*-amyl alcohol and stirred at 95°C for 96 h in a condenser-flask system. After cooling to room temperature and centrifugation at 6,000 rpm for 30 min, the supernatant was either purified for elemental analysis (see below) or combined with 15 mL of iodomethane and stirred in a sealed condenser-flask system at 60°C for 24 h. The quaternary ammonium polycation was precipitated from this solution with an excess of ethyl acetate, collected by vacuum filtration, washed with additional ethyl acetate, and then kept under vacuum overnight to remove residual solvent (14, 16) to yield 12.2 g of *N,N*-dodecyl,methyl-PEI.

N-Dodecyl-PEI was purified from the above-referenced reaction mixture prior to the methylation by dialysis within a regenerated cellulose membrane (Spectrum Labs, 3.5-kDa molecular weight cutoff) against 2 L of hexane for 24 h thrice, followed by solvent removal under vacuum. Elemental analysis, performed by Columbia Analytical Labs, yielded a C:H:N of 72.3:12.8:4.0 by weight (or 21.1:44.5:1.0 by mol).

The hydrophobic polycationic coating was applied by brush-coating slides from a 50 mg/mL solution of *N,N*-dodecyl,methyl-PEI in chloroform with a 3/8 inch nylon-bristled paint brush (Loew-Cornell) and allowing it to dry in a chemical hood. This painting procedure was repeated twice more. The square 2.5 x 2.5-cm slides used were cleaned by sonication in isopropyl alcohol for 5 min, followed by autoclaving. Glass slides were cut from standard microscope slides (VWR International), while low-density polyethylene and polypropylene slides were cut from 12" x 12" x 1/16" sheets (McMaster-Carr Supply Co.).

Virus culture and ribonuclease pretreatment

The influenza A/WSN/33 (H1N1) virus was cultured from Madin-Darby canine kidney (MDCK) cells as described previously (14). Sucrose-gradient purified influenza A/PR/8/34 (H1N1) suspended in HEPES-saline buffer was used as obtained from Charles River Laboratories. Wild-type and zanamivir-resistant influenza A/MN/833/80 (H4N2) viruses were obtained from egg allantoic fluid as described previously (15).

Exogenous viral RNA (single- and double-stranded) was digested in all viral samples by incubating 100 μ L of an influenza virus solution with 15 μ L of ribonuclease III buffer, 50 μ L of ribonuclease III enzyme (1 U/ μ L, Ambion AM2290), and 5 μ L of 1000-fold-diluted ribonuclease A (3,500 U/ μ L, Invitrogen 12091-021) in (phosphate-buffered saline) PBS for 1 h at 37°C (18-20). Subsequently, 5 μ L of Anti-ribonuclease (20 U/ μ L, Ambion AM2690) was added, and the solution was incubated at room temperature for 15 min before being placed on ice.

A 10- μ L droplet of a viral aqueous solution was sandwiched between two slides (glass, polyethylene, or polypropylene) in a 6 x 1.5 cm a round polystyrene Petri dish. After a 5-min incubation at room temperature, the slides were separated and washed with 990 μ L of PBS.

Viral samples were collected either prior to contact with slides, after contact with bare slides, or after contact with polycation-coated slides (16).

Plaque assays were used to quantify the infectious viral particles (in pfu/mL) in solution by infecting a monolayer of MDCK cells in 6-well plates with 200 μ L of a viral solution (16).

ELISA

An enzyme-linked immunosorbent assay (ELISA) of influenza virus nucleoprotein (NP) was performed with a 96-well maxisorp immunoplate (Nunc International) as follows: the wells were incubated with 100 μ L of a 1:1,000 dilution of goat anti-influenza A polyclonal antibody (AB1074, Millipore Corp.) in PBS at 4°C overnight and then washed thrice with 100 μ L of a solution of 0.2% (w/v) I-block (Applied Biosystems) and 0.05% Tween 20 (v/v) in PBS (PBST), followed by a further incubation with an additional 100 μ L of PBST for 3 h at room temperature. Then 100- μ L volumes of viral samples, prepared by combining equal volumes of virus solution and 2X PBST were added. After incubation overnight at 4°C, the wells were washed thrice with 100 μ L of PBST and incubated with 100 μ L of a 3:10,000 dilution of mouse anti-influenza A biotinylated monoclonal antibody (MAB8257B, Millipore Corp.) in PBST for 3 h at room temperature. This was followed by washing thrice with 100 μ L of PBST and incubation with 100 μ L of a 1:200 dilution of a streptavidin-horseradish peroxidase conjugate (18-152, Millipore Corp.) in PBS for 2 h at room temperature before washing thrice with 100 μ L of PBST. Colorimetric development of 50 μ L of 1-Step Ultra TMB (Thermo Scientific) at room temperature was stopped with 50 μ L of 0.2 M H₂SO₄ after incubation for 12 min, 6 min, 9 min, or 4 min with WSN, PR8L, TurkWt, or TurkMu influenza virus strains, respectively. Light absorbances measured at 450 nm for virus samples prior to assay, as well as after contact with

bare slides or with *N,N*-dodecyl,methyl-PEI-coated slides, were referenced to standard curves constructed from serially-diluted stock samples and normalized to their plaque-assay determined titers.

SDS-PAGE

Sucrose-gradient purified PR8H viral samples were disrupted with 1% (w/v) sodium dodecylsulfate (SDS) in PBS such that the final concentration was 0.1% SDS. Proteins from viral samples were concentrated and washed using Amicon Ultra 0.5-mL microcentrifuge filters (10-kDa molecular weight cutoff, Millipore Corp.), according to the manufacturer's instructions. Briefly, proteins were concentrated at room temperature by centrifugation at 14,000 x g and then washed thrice with 400 μ L of 0.1% SDS in PBS by additional centrifugation. The final 14.0 μ L of washed and concentrated protein solution was run on a SDS-PAGE using a 7% Tris-acetate NuPAGE gel (Invitrogen) and Tris-acetate buffer kit (Invitrogen) according to manufacturer's instructions. Briefly, 14.0 μ L of concentrated protein was combined with 5.4 μ L of 4X lithium dodecylsulfate sample buffer, and 2.2 μ L of 10X reducing agent prior to incubation at 70°C for 10 min. The prepared samples and a boiled protein ladder (10-250 kDa, New England BioLabs) were added to the gel and subjected to electrophoresis for 60 min at 150 V. The resultant gel was stained with SimplyBlue comassie blue stain (Invitrogen) and imaged on an Alpha Imager 2200 (Cell Biosciences). Gel scanning densitometry analysis was performed using ImageJ software (NIST) by calibrating the measured pixel density to optical density and then developing a standard curve with a power-law fit using the protein bands of serially-diluted viral samples to which assay samples were referenced. Assignment of protein bands was based on the literature data (4, 35).

Viral RNA extraction and quantification with qRT-PCR

RNA was extracted from 200 μL of a viral solution using the PureLink viral RNA/DNA kit (Invitrogen) according to manufacturer's instructions giving a final 110 μL of viral RNA, stored at -80°C . Quantification was performed with the RNA Ultrasense qRT-PCR mix (Invitrogen) according to manufacturer's instructions. The primers and probe (IDT) sequences used were identical to those previously developed (17). Real-time reverse transcriptase (RT) PCR was performed on an Applied Biosystems 7500 real-time PCR system under the following cycling conditions: 50°C for 15 min, 95°C for 2 min, and then 50 cycles of 95°C for 15 sec and 60°C for 32 sec. RNA samples from virus prior to assay, after contact with bare slides, and after contact with polycation-coated slides were referenced to standard curves constructed from serially-diluted stock samples and normalized to plaque assay titers (Applied Biosystems 7500 Software v2.0.1). All samples and standard curves were included on the same reaction plate.

RT-PCR and sequencing

Aliquots of 200 μL of WSN virus strain samples prior to assay and after contact with *N,N*-dodecyl,methyl-PEI-coated slides underwent RNA extraction as described above. Reverse transcription was performed using the Omniscript RT Kit (Qiagen) according to manufacturer's instructions with Anti-ribonuclease (20 U/ μL , Ambion AM2690) as the ribonuclease inhibitor with the aforementioned primers (IDT) (17). For amplification of the newly transcribed viral DNA, the TopTaq DNA Polymerase (Qiagen) with a dNTP mix (Promega) and primers were used according to manufacturer's instructions. Sequencing was performed by the MIT Biopolymers Facility.

Detergent studies

The viability of MDCK cells after a 1-h incubation at room temperature with 100 μL of serially diluted dodecyltrimethylammonium bromide (DTAB) in PBS was determined using the CellTiter96 Aqueous Non-radioactive Cell Proliferation Assay (Promega), an MTS-based assay for mitochondrial activity (36), and was performed according to manufacturer's instructions. The measured 50% toxicity concentration (TC_{50}) of DTAB was calculated using replicates of dose-response fitted curves (Origin Labs OriginPro v8.1).

The 50% inhibitory concentration (IC_{50}) of DTAB against PR8 was measured by incubating serial dilutions of detergent with PR8 for 30 min at room temperature prior to determination of their infectivity by plaque assay (16, 25). Plaques were easily identifiable at and below 43 $\mu\text{g}/\text{mL}$ DTAB, while above this level (e.g., at 85 $\mu\text{g}/\text{mL}$) cells were opaque, thus making potential plaques indistinguishable. Hence the IC_{50} value was calculated using replicates of dose-response fitted curves (Origin Labs OriginPro v8.1) to DTAB concentrations not exceeding 43 $\mu\text{g}/\text{mL}$.

Scanning electron microscopy (SEM)

Plain and *N,N*-dodecyl,methyl-PEI-coated square silicon wafers (1 cm x 1 cm) were placed in a Petri dish, and a 10- μl droplet of an influenza virus solution was placed in the center before sandwiching with a plain silicon wafer to spread the droplet. This system was incubated at room temperature for 30 min before fixing the samples with Karnovsky's fixative kit (Polysciences cat. no. 22872-5). To this end, the samples were incubated in the fixing solution (2% paraformaldehyde and 2.5% glutaraldehyde in 0.1 M sodium phosphate buffer) for 2 h and

rinsed for 10 min in fresh phosphate buffer. The samples were then incubated in the dark in a 1% osmium tetroxide solution (Sigma cat. no. 75632) for 1 h before sequentially rinsing in 35%, 50%, 70%, 95%, and 100% aqueous ethanol solutions for 10 min each, followed by dehydration thrice in 100% ethanol. The samples were then freeze-dried in liquid nitrogen and sputter-coated before imaging with a scanning electron microscope (JEOL JSM-6700F) at a 100,000X magnification.

4.5 References

1. Beaglehole R, Irwin A, Prentice T (2004) *The World Health Report: Changing History* (World Health Organization, Geneva).
2. Garibaldi RA (1985) Epidemiology of community-acquired respiratory tract infections in adults: Incidence, etiology, and impact. *Am J Med* 78:32-37.
3. Dushoff J, Plotkin JB, Viboud C, Earn DJD, Simonsen L (2006) Mortality due to influenza in the United States—An annualized regression approach using multiple-cause mortality data. *Am J Epidemiol* 163:181-187.
4. Lamb RA, Krug RM (2006) *Fields Virology*, eds Knipe DM & Howley PM (Lippincott, Philadelphia), 5th Ed, pp 1488-1531.
5. Scholtissek C (1994) Source for influenza pandemics. *Eur J Epidemiol* 10:455-458.
6. Osterholm MT (2005) Preparing for the next pandemic. *N Engl J Med* 352:1839-1842.
7. Wright PF (2008) Vaccine preparedness — are we ready for the next influenza pandemic? *N Engl J Med* 358:2540-2543.
8. Weinstock DM, Zuccotti G (2009) The evolution of influenza resistance and treatment. *J Am Med Assoc* 301:1066-1069.
9. Boyce JM, Potter-Bynoe G, Chenevert C, King T (1997) Environmental contamination due to methicillin-resistant *Staphylococcus aureus*: Possible infection control implications. *Infect Cont Hosp Ep* 18:622-627.
10. Rosenthal VD, *et al.* (2006) Device-associated nosocomial infections in 55 intensive care units of 8 developing countries. *Ann Intern Med* 145:582-591.
11. Klibanov AM (2007) Permanently microbicidal materials coatings. *J Mater Chem* 17:2479-2482.
12. Lin J, Qiu SY, Lewis K, Klibanov AM (2003) Mechanism of bactericidal and fungicidal activities of textiles covalently modified with alkylated polyethylenimine. *Biotechnol Bioeng* 83:168-172.
13. Mukherjee K, Rivera JJ, Klibanov AM (2008) Practical aspects of hydrophobic polycationic bactericidal "paints". *Appl Biochem Biotechnol* 151:61-70.
14. Haldar J, An DQ, de Cienfuegos LA, Chen JZ, Klibanov AM (2006) Polymeric coatings that inactivate both influenza virus and pathogenic bacteria. *Proc Natl Acad Sci USA* 103:17667-17671.
15. Haldar J, Chen J, Tumpey TM, Gubareva LV, Klibanov AM (2008) Hydrophobic polycationic coatings inactivate wild-type and zanamivir- and/or oseltamivir-resistant human and avian influenza viruses. *Biotechnol Lett* 30:475-479.
16. Haldar J, Weight AK, Klibanov AM (2007) Preparation, application and testing of permanent antibacterial and antiviral coatings. *Nature Protoc* 2:2412-2417.
17. van Elden LJR, Nijhuis M, Schipper P, Schuurman R, van Loon AM (2001) Simultaneous detection of influenza viruses A and B using real-time quantitative PCR. *J Clin Microbiol* 39:196-200.
18. Majde JA, Guha-Thakurta N, Chen Z, Bredow S, Krueger JM (1998) Spontaneous release of stable viral double-stranded RNA into the extracellular medium by influenza virus-infected MDCK epithelial cells: implications for the viral acute phase response. *Arch Virol* 143:2371-2380.
19. Nuanualsuwan S, Cliver DO (2002) Pretreatment to avoid positive RT-PCR results with inactivated viruses. *J Virol Methods* 104:217-225.

20. Weber F, Wagner V, Rasmussen SB, Hartmann R, Paludan SR (2006) Double-stranded RNA is produced by positive-strand RNA viruses and DNA viruses but not in detectable amounts by negative-strand RNA viruses. *J Virol* 80:5059-5064.
21. Ewing B, Hillier L, Wendl MC, Green P (1998) Base-calling of automated sequencer traces using phred. I. Accuracy assessment. *Genome Res* 8:175-185.
22. Akinc A, Thomas M, Klibanov AM, Langer R (2005) Exploring polyethylenimine-mediated DNA transfection and the proton sponge hypothesis. *J Gene Med* 7:657-663.
23. Thomas M, Lu JJ, Ge Q, Zhang CC, Chen JZ, Klibanov AM (2005) Full deacylation of polyethylenimine dramatically boosts its gene delivery efficiency and specificity to mouse lung. *Proc Natl Acad Sci USA* 102:5679-5684.
24. Neamark A, Suwanton O, Bahadur KCR, Hsu CYM, Supaphol P, Uludag H (2009) Aliphatic lipid substitution on 2 kDa polyethylenimine improves plasmid delivery and transgene expression. *Mol Pharm* 6:1798-1815.
25. Hayden FG, Cote KM, Douglas RG (1980) Plaque inhibition assay for drug susceptibility testing of influenza-viruses. *Antimicrob Agents Chemother* 17:865-870.
26. Vieira OV, Hartmann DO, Cardoso CMP, Oberdoerfer D, Baptista M, Santos MAS, Almeida L, Ramalho-Santos J, Vaz WLC (2008) Surfactants as microbicides and contraceptive agents: a systematic *in vitro* study. *PLoS ONE* 3:1-12.
27. Abe M, Kaneko K, Ueda A, Otsuka H, Shiosaki K, Nozaki C, Goto S (2007) Effects of several virucidal agents on inactivation of influenza, newcastle disease, and avian infectious bronchitis viruses in the allantoic fluid of chicken eggs. *Jpn J Infect Dis* 60:342-346.
28. Armstrong JA, Froelich EJ (1964) Inactivation of viruses by benzalkonium chloride. *Appl Microbiol* 12:132-137.
29. Oxford JS, Potter CW, McLaren C, Hardy W (1971) Inactivation of influenza and other viruses by a mixture of virucidal compounds. *Appl Microbiol* 21:606-610.
30. Kabanov VA, Yaroslavov AA (2002) What happens to negatively charged lipid vesicles upon interacting with polycation species? *J Control Release* 78:267-271.
31. Ikeda T, Lee B, Yamaguchi H, Tazuke S (1990) Time-resolved fluorescence anisotropy studies on the interaction of biologically-active polycations with phospholipid-membranes. *Biochim Biophys Acta* 1021:56-62.
32. Polozov IV, Bezrukov L, Gawrisch K, Zimmerberg J (2008) Progressive ordering with decreasing temperature of the phospholipids of influenza virus. *Nat Chem Biol* 4:248-255.
33. Scheiffele P, Rietveld A, Wilk T, Simons K (1999) Influenza viruses select ordered lipid domains during budding from the plasma membrane. *J Biol Chem* 274:2038-2044.
34. Rothman JE, Tsai DK, Dawidowicz EA, Lenard J (1976) Transbilayer phospholipid asymmetry and its maintenance in membrane of influenza-virus. *Biochemistry* 15:2361-2370.
35. Shaw ML, Stone KL, Colangelo CM, Gulcicek EE, Palese P (2008) Cellular proteins in influenza virus particles. *PLoS Pathog* 4:1-13.
36. Mosmann T (1983) Rapid colorimetric assay for cellular growth and survival: Application to proliferation and cytotoxicity assays. *J Immunol Methods* 65:55-63.

Appendix I.

Figure A. Determination of the efficacy of ribonuclease-catalyzed digestion of RNA and of its subsequent inhibition by means of real-time reverse-transcription PCR. Amplification curves represent (a) influenza viral (WSN strain) RNA, (b) viral RNA subjected to ribonuclease digestion and then inhibition, (c) addition of fresh RNA to the ribonuclease digestion mixture, and (d) RNA-free aqueous solution. For (a), (b), (c), and (d) the Y-axes are offset for clarity by 0.15, 0.10, 0.05, and 0.00 units, respectively.

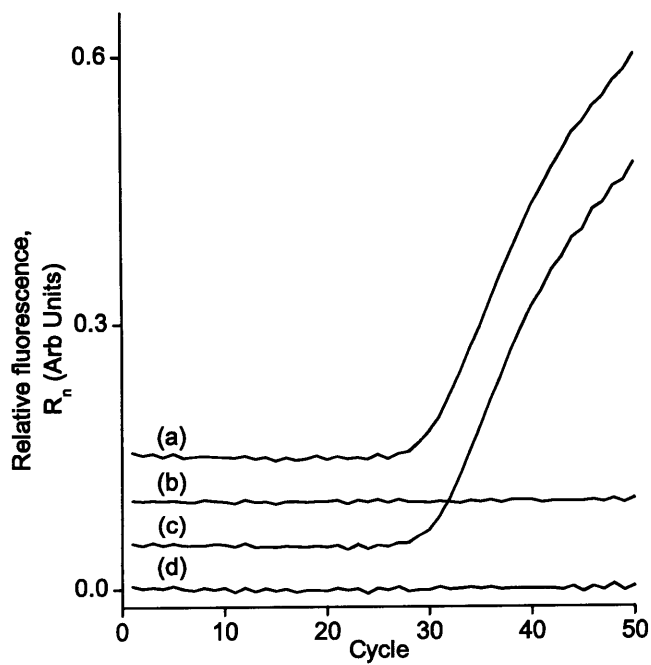
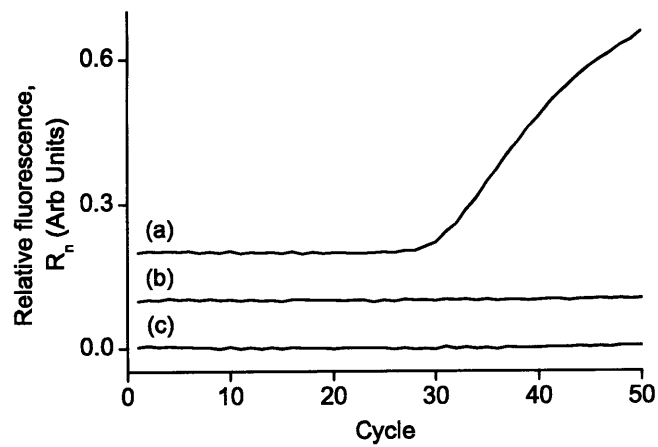


Figure B. Determination of putative non-specific amplification of the *N,N*-dodecyl,methyl-PEI coating with real-time reverse-transcription PCR. Amplification curves represent (a) influenza viral (WSN strain) RNA, (b) PBS incubated with polycation-coated polyethylene slides, and (c) RNA-free aqueous solution. For (a), (b), and (c) the Y-axes are offset for clarity by 0.2, 0.1, and 0.0 units, respectively.



Acknowledgements

I would like to thank Professor Alexander Klibanov for his advice and research opportunity. His availability and personal insights into research significantly accelerated my development as a scientist, for which I will always be grateful. In addition, I would like to thank my committee member and collaborator, Professor Jianzhu Chen, whose virology expertise has been instrumental in my influenza studies. I am also greatly thankful to my thesis committee chair, Professor Alice Ting, who was a great help throughout.

This work would not have been possible without the help from my colleagues. I've received immeasurable assistance from current and former Klibanov lab members: Eugene Antipov, Koushik Mukjeree, Jaime Rivera, Jayanta Haldar, Jie Ouyang, Jessie Wong, Jaimie Lee, Wei Du, Jennifer Fortune, Alisha Weight, Alyssa Larson, Roger Nassar, and of course to my undergraduate researcher, Peter Tieu. Members outside of the lab that have been enormously helpful include Liguu Wu, Carol McKinley, Steve Chen, Zhuyan Guo, Ching-Hung Shen, Sebastien Gouin, and Laura Jennings.

Finally I would like to thank my family for their love and support.